

# A Mixture Transition Distribution Modeling for Higher-Order Circular Markov Processes

Hiroaki Ogata<sup>\*1</sup> and Takayuki Shiohama<sup>†2</sup>

<sup>1</sup>Faculty of Economics and Business Administration, Tokyo Metropolitan University

<sup>2</sup>Department of Data Science, Nanzan University

## Abstract

The stationary higher-order Markov process for circular data is considered by employing the mixture transition distribution (MTD) modeling. The underlying circular transition distribution is based on Wehrly and Johnson's bivariate joint circular models. The structures of the circular autocorrelation function together with the circular partial autocorrelation function are investigated and found to be similar to those of the autocorrelation and partial autocorrelation functions of the real-valued autoregressive process when the underlying binding density has zero sine moments. The validity of the model is assessed by applying it to some Monte Carlo simulations and real directional data.

**keywords:** circular statistics, Markov process, maximum likelihood estimation, spectral density; stationary process, time series analysis

MSC2020: 60G10, 60J05, 62M05.

---

<sup>\*</sup>1-1 Minami-Osawa, Hachioji, Tokyo, 192-0397, Japan. [hiroakiogata@tmu.ac.jp](mailto:hiroakiogata@tmu.ac.jp)

<sup>†</sup>18 Yamazato-cho, Showa, Nagoya, 466-8673, Japan.

# 1 Introduction

Statistical analysis related to the data that take values on unit vectors is called directional statistics, where the direction is more important than the magnitude. Directional data occurs in many areas, namely geostatistics, natural sciences, environmental sciences, biology, information science, genetics, and among others. The basic manifold of the high dimensional sphere is the unit circle which is embedded in the Euclidean space  $\mathbb{R}^2$ , and the statistical methods for the unit circle are known as circular statistics. For further reviews, we refer to the monographs of [Jammalamadaka and SenGupta \(2001\)](#), [Mardia and Jupp \(2009\)](#), and [Pewsey et al. \(2013\)](#). In addition, a recent review paper of [Pewsey and García-Portugués \(2021\)](#) should be added.

While many data taking values on the unit circle or sphere are characterized by time series structure, the statistical analysis for circular time series is not fully developed so far. We can observe many time series data on the circle, such as the wind or wave directions, time records of a certain event, and animal movement trajectories, which show typical periodic patterns. As for the correlation coefficient of the bivariate circular data, [Fisher and Lee \(1983, 1994\)](#) proposed circular correlation coefficients and considered basic circular time series models as linked autoregressive and moving average models and wrapping processes for real-valued time series. A comprehensive analysis of circular time series modeling can be found in [Breckling \(1989\)](#).

One of the major approaches for modeling circular time series is to apply the Markov models on it. [Wehrly and Johnson \(1980\)](#) proposed joint distribution for the circular random variables. [Holzmann et al. \(2006\)](#) applied it for time series modeling using Hidden Markov models. [Abe et al. \(2017\)](#) showed the circular autocorrelation structure of the circular Markov process proposed by [Wehrly and Johnson \(1980\)](#). Another Markov-based circular time series is considered by [Kato \(2010\)](#) where he considered the Möbius transformation of the circular random variables to produce the transition densities. His models are extended by [Jones et al. \(2015\)](#), where they considered the circular joint distributions called ‘circulas’ for analyzing correlated structures for circular random variables.

Whilst all these approaches are based on the first-order Markov modeling for circular time series, investigating higher-order Markov models on the circle is of primary importance. It is worthwhile to mention that, as far as the authors’ knowledge, there exist no approaches for higher-order circular Markov models in the literature. The statistical modeling with real-valued time series, [Raftery \(1985\)](#) considered the higher-order Markov modeling by using a mixture of transition densities (MTD), and his models are lately developed to the MTD modeling for a higher-order dependency of the observed time series, see for details, [Raftery and Tavaré \(1994\)](#), [Le et al. \(1996\)](#), and [Berchtold and Raftery \(2002\)](#). In this pa-

per, we develop the higher-order Markov process on the circle using the transition density of [Wehrly and Johnson \(1980\)](#)'s model together with the MTD approaches. The maximum likelihood estimation for the model parameters is introduced and some information criteria for model selections are discussed.

The rest of the paper is organized as follows. Section 2 introduces our proposed higher-order Markov process on the circle by incorporating MTD modeling approaches. The first- and second-order stationarity of the process is investigated. The circular autocorrelation (CACF) and circular partial autocorrelation function (CPACF) are derived in Section 3. Moreover, the spectral density function of the higher-order circular time series is also given. In Section 4, for the unknown parameter estimation, the maximum likelihood estimator (MLE) is investigated. We provide asymptotic normality of the MLE. Section 5 illustrates some finite sample performances of MLE via Monte Carlo simulations. Real data analysis is conducted in Section 6. Finally, Section 7 concludes our paper. All the proofs of theorems and lemmas are given in Appendix A.

## 2 Mixture Transition Distribution Models on a Circle

We consider the circular strictly stationary process  $\{\Theta_t\}_{t \in \mathbb{Z}}$ . Throughout the paper, we use the notation  $\theta_{a:b} = \{\theta_a, \theta_{a-1}, \dots, \theta_{b+1}, \theta_b\}$  for the  $\sigma$ -field generated by the random variables  $\{\Theta_t\}$ ,  $t \in \{a, a-1, \dots, b+1, b\}$  for  $a \geq b$ . The transition density for the Markov process on the circle proposed by [Wehrly and Johnson \(1980\)](#) was set as

$$f(\theta_t | \theta_{t-1: -\infty}) = f(\theta_t | \theta_{t-1}) = 2\pi g[2\pi\{F(\theta_t) - qF(\theta_{t-1})\}]f(\theta_t). \quad (1)$$

Here,  $f$  and  $g$  are densities on the circle,  $F(\theta) = \int_0^\theta f(\xi)d\xi$  is a distribution function, and  $q \in \{-1, 1\}$  is a non-random factor which determines the sign of  $F(\theta_{t-1})$  and the direction of the association of consecutive sequences. The  $f$  corresponds to the marginal density function of  $\Theta_t$ . If we set the marginal as the circular uniform,  $f(\theta_t) = 1/(2\pi)$ , the above transition density has a simpler form:

$$f(\theta_t | \theta_{t-1}) = g(\theta_t - q\theta_{t-1}). \quad (2)$$

The density  $g$  is sometimes called a binding density as in [Jones et al. \(2015\)](#).

Now, we extend the circular Markov process proposed by [Wehrly and Johnson \(1980\)](#) to a higher-order Markov process. To this end, we employ the mixture transition distribution (MTD) model which originates in [Raftery \(1985\)](#). We use the term  $p$ th-order Markov process, indicating that the conditional distribution is determined by only  $p$  adjacent past values. Referring to (2), we define the circular  $p$ th-order mixture transition distribution model by

setting the transition density as

$$f(\theta_t|\theta_{t-1:-\infty}) = f(\theta_t|\theta_{t-1:t-p}) = \sum_{i=1}^p a_i g(\theta_t - q_i \theta_{t-i}). \quad (3)$$

Here  $g(\cdot)$  is any circular density functions,  $a_i$  ( $i = 1, \dots, p-1$ )  $\geq 0$  and  $a_p > 0$  are non negative and positive constants, respectively. The sum of mixing weights must satisfy  $\sum_{i=1}^p a_i = 1$  and  $q_i$ 's are constants that take the values  $-1$  or  $1$ . Hereafter, we call model (3) an MTD-AR( $p$ ) model.

**Assumption 1.** *The binding density  $g$  has the following  $m$ -th trigonometric moment as*

$$E[\exp(im\Theta)] = \rho_m e^{i\mu_m},$$

where  $i$  is an imaginary unit defined as  $i^2 = -1$ ,  $\rho_m \in (0, 1)$  and  $\mu_m \in [-\pi, \pi)$  are the  $m$ -th order mean resultant length and mean direction, respectively.

When  $m = 1$  and  $q_1 = 1$ , the mean direction  $\mu_1$  determines the local trend or direction of the movement in angular around the previous direction  $\theta_{t-1}$  with concentration  $\rho_1$ . For the case with  $q_1 = -1$ , describing the role of the parameter  $\mu_1$  is difficult to interpret.

The lag  $i$ -th component in equation (3) becomes  $a_i g(\theta_t - q_i \theta_{t-i})$ , and the corresponding  $m$ -th conditional trigonometric moment of  $\Theta_t$  given  $\Theta_{t-i} = \theta_{t-i}$  becomes

$$E \left[ \begin{pmatrix} \cos m\Theta_t \\ \sin m\Theta_t \end{pmatrix} \middle| \Theta_{t-i} = \theta_{t-i} \right] = D_m Q_i \begin{pmatrix} \cos m\theta_{t-i} \\ \sin m\theta_{t-i} \end{pmatrix},$$

where

$$D_m = \rho_m \begin{pmatrix} \cos \mu_m & -\sin \mu_m \\ \sin \mu_m & \cos \mu_m \end{pmatrix} \quad \text{and} \quad Q_i = \begin{pmatrix} 1 & 0 \\ 0 & q_i \end{pmatrix}.$$

Here, the matrix  $Q_i$  determines the direction of the association between  $\Theta_t$  and  $\Theta_{t-i}$ . See Lemma 1 in Appendix for derivation. The matrix  $D_m$  plays an important role in determining the autocorrelation structures of the Markov processes.

## 2.1 First- and second-order stationarity

Note that the process is said to be second-order stationary if its first and second moments are all independent of the time  $t$ . First, we consider the conditions for the process  $\{\mathbf{U}_t = (\cos \Theta_t \ \sin \Theta_t)^T\}_{t \in \mathbb{Z}}$  to be the first-order stationary. Let us denote  $\boldsymbol{\mu}_t = E(\mathbf{U}_t)$ , and  $\mathbf{m}_t = (\boldsymbol{\mu}_t^T, \dots, \boldsymbol{\mu}_{t-p+1}^T)^T$ . Then,

$$\boldsymbol{\mu}_t = E[E(\mathbf{U}_t | \Theta_{t-1:t-p})] = E \left[ \sum_{i=1}^p a_i D_1 Q_i \mathbf{U}_{t-i} \right] = \sum_{i=1}^p a_i D_1 Q_i \boldsymbol{\mu}_{t-i}.$$

For the detailed derivation of this expression, see Lemma 1 in Appendix. In matrix form, this is written by

$$\mathbf{m}_t = \begin{pmatrix} \boldsymbol{\mu}_t \\ \boldsymbol{\mu}_{t-1} \\ \vdots \\ \boldsymbol{\mu}_{t-p+1} \end{pmatrix} = \begin{pmatrix} a_1 D_1 Q_1 & \cdots & a_{p-1} D_1 Q_{p-1} & a_p D_1 Q_p \\ I_2 & \cdots & O & O \\ \vdots & \ddots & \vdots & \vdots \\ O & \cdots & I_2 & O \end{pmatrix} \begin{pmatrix} \boldsymbol{\mu}_{t-1} \\ \boldsymbol{\mu}_{t-2} \\ \vdots \\ \boldsymbol{\mu}_{t-p} \end{pmatrix} =: \mathbf{A} \mathbf{m}_{t-1}, \quad (4)$$

where  $I_2$  denotes the  $2 \times 2$  identity matrix. Following the proof of Theorem 1 in Le et al. (1996), we find that if and only if all the absolute value of the eigenvalues of  $2p \times 2p$  matrix  $\mathbf{A}$  defined by equation (4) are less than 1, then the process  $\{\mathbf{U}_t\}_{t \in \mathbb{Z}}$  is first-order stationary. The required condition for the first-order stationarity is that all the roots of the characteristic equation

$$\det(\lambda^p I_2 - \lambda^{p-1} a_1 D_1 Q_1 - \cdots - a_p D_1 Q_p) = 0$$

lie in the unit circle.

**Remark 1** (MTD-AR(1) case). The first-order stationary condition is the absolute values of the eigenvalues of  $D_1$  are both less than 1. Recall that  $a_1 = 1$  if  $p = 1$  by definition. The characteristic polynomial is

$$\begin{aligned} \det(\lambda I_2 - D_1 Q_1) &= \det \begin{pmatrix} \lambda - \rho_1 \cos \mu_1 & q_1 \rho_1 \sin \mu_1 \\ -\rho_1 \sin \mu_1 & \lambda - q_1 \rho_1 \cos \mu_1 \end{pmatrix} \\ &= \lambda^2 - (q_1 + 1) \rho_1 \cos \mu_1 \cdot \lambda + q_1 (\rho_1)^2. \end{aligned}$$

The roots of the characteristic equation are  $\rho_1(\cos \mu_1 \pm i \sin \mu_1)$  for  $q_1 = 1$  and  $\pm \rho_1$  for  $q_1 = -1$ . For both cases with  $q_1 = \pm 1$ , the absolute values of the roots are less than 1 unless the distribution  $g$  degenerates. Assumption 1 ensures that the process is first-order stationary.

**Remark 2** (MTD-AR(2) case). For the MTD-AR(2) model, the characteristic polynomial becomes

$$\begin{aligned} \det(\lambda^2 I_2 - \lambda a_1 D_1 Q_1 - a_2 D_1 Q_2) &= \lambda^4 - (q_1 + 1) a_1 \rho_1 \cos \mu_1 \lambda^3 \\ &+ (q_1 a_1^2 \rho_1^2 - (q_2 + 1) a_2 \rho_1 \cos \mu_1) \lambda^2 + 2 a_1 a_2 \rho_1^2 \lambda + a_2^2 \rho_1^2 (q_1 \cos^2 \mu_1 + q_2 \sin^2 \mu_1). \end{aligned} \quad (5)$$

Hence the roots of (5) can be uniquely determined when the density function  $g$  is specified, and the absolute values of the resulting roots are less than unity, which indicates the MTD-AR(2) model is always first-order stationary.

Next, we consider second-order stationarity of the process  $\{\mathbf{U}_t\}_{t \in \mathbb{Z}}$ . Let us denote  $V_t = E(\mathbf{U}_t \mathbf{U}_t^T)$ . Then,

$$\begin{aligned}
V_t &= E \left[ E \left\{ \begin{pmatrix} \cos^2 \Theta_t & \cos \Theta_t \sin \Theta_t \\ \sin \Theta_t \cos \Theta_t & \sin^2 \Theta_t \end{pmatrix} \middle| \Theta_{t-1:t-p} \right\} \right] \\
&= E \left[ E \left\{ \frac{1}{2} I_2 + \frac{1}{2} \begin{pmatrix} \cos 2\Theta_t & \sin 2\Theta_t \\ \sin 2\Theta_t & -\cos 2\Theta_t \end{pmatrix} \middle| \Theta_{t-1:t-p} \right\} \right] \\
&= E \left[ \frac{1}{2} I_2 + \frac{1}{2} \sum_{i=1}^p a_i D_2 Q_i \begin{pmatrix} \cos 2\Theta_{t-i} & \sin 2\Theta_{t-i} \\ \sin 2\Theta_{t-i} & -\cos 2\Theta_{t-i} \end{pmatrix} Q_i \right] \\
&= \frac{1}{2} (I_2 - D_2) + D_2 \sum_{i=1}^p a_i Q_i V_{t-i} Q_i. \tag{6}
\end{aligned}$$

For the above derivation, we use Lemma 2 in Appendix for the calculation of the conditional expectation. Define the following  $2p \times 2p$  block matrices:

$$\begin{aligned}
\mathcal{V}_t &= \begin{pmatrix} V_t & & & \\ & V_{t-1} & & \\ & & \ddots & \\ & & & V_{t-(p-1)} \end{pmatrix}, \quad \mathcal{D} = \begin{pmatrix} D_2 & O & \cdots & O \\ O & I_2 & \cdots & O \\ \vdots & \vdots & \ddots & \vdots \\ O & O & \cdots & I_2 \end{pmatrix}, \\
\mathcal{Q} &= \begin{pmatrix} \sqrt{a_1} Q_1 & \cdots & \sqrt{a_{p-1}} Q_{p-1} & \sqrt{a_p} Q_p \\ I_2 & \cdots & O & O \\ \vdots & \ddots & \vdots & \vdots \\ O & \cdots & I_2 & O \end{pmatrix},
\end{aligned}$$

and  $2p \times 2$  block matrix

$$\mathcal{C} = \left( \frac{1}{2} (I_2 - D_2^T) \quad O \quad \cdots \quad O \right)^T.$$

Then, (6) is written as

$$\mathcal{V}_t = \mathcal{D} \mathcal{Q} \mathcal{V}_{t-1} \mathcal{Q}^T + \mathcal{C}. \tag{7}$$

Using vec operator and Kronecker product, (7) is written as

$$\text{vec}(\mathcal{V}_t) = (\mathcal{Q} \otimes \mathcal{D} \mathcal{Q}) \text{vec}(\mathcal{V}_{t-1}) + \text{vec}(\mathcal{C}).$$

The second-order stationarity of  $\mathbf{U}_t$  requires that all of the absolute values of the eigenvalues of the  $4p^2 \times 4p^2$  matrix  $\mathcal{Q} \otimes \mathcal{D} \mathcal{Q}$  are less than 1. The eigenvalues of  $\mathcal{Q} \otimes \mathcal{D} \mathcal{Q}$  are of the form  $\lambda_i \nu_j$  where  $\lambda_i$  and  $\nu_j$  are eigenvalues of  $\mathcal{Q}$  and  $\mathcal{D} \mathcal{Q}$ . If  $|\lambda_i| < 1$  and  $|\nu_j| < 1$  for all  $i$  and  $j$ , all the eigenvalues of  $\mathcal{Q} \otimes \mathcal{D} \mathcal{Q}$  are inside the unit circle. Hence, the required condition for the second-order stationarity is similar to that of the first-order condition and is the product of

all the combinations of the absolute values of the root of the equations

$$\det(\lambda^p I_2 - \lambda^{p-1} a_1^{1/2} Q_1 - \dots - a_p^{1/2} Q_p) = 0$$

and

$$\det(\lambda^p I_2 - \lambda^{p-1} a_1^{1/2} D_2 Q_1 - \dots - a_p^{1/2} D_2 Q_p) = 0$$

are less than unity.

**Remark 3** (MTD-AR(1) case). From the equations  $\det(\lambda I_2 - Q_1) = 0$ , we obtain eigenvalues as 1 and  $q_1$ , which lie on the unit circle. Hence, for the second-order stationarity, we need that the eigenvalues of  $\det(\lambda I_2 - D_2 Q_1)$  are both less than 1. The characteristic polynomial is

$$\begin{aligned} \det(\lambda I_2 - D_2 Q_1) &= \det \begin{pmatrix} \lambda - \rho_2 \cos \mu_2 & q_1 \rho_2 \sin \mu_2 \\ -\rho_2 \sin \mu_2 & \lambda - q_1 \rho_2 \cos \mu_2 \end{pmatrix} \\ &= \lambda^2 - \rho_2 \cos \mu_2 (1 + q_1) \lambda + q_1 \rho_2^2. \end{aligned}$$

Since the roots of the characteristic equation are  $\rho_2(\cos \mu_2 \pm i \sin \mu_2)$  if  $q_1 = 1$  and  $\pm \rho_2$  if  $q_1 = -1$ . For both cases, the roots are less than 1, the process is always second-order stationary.

### 3 Time Series Structures for Circular Data

We begin with reviewing the measure of association between two circular random variables  $\Theta$  and  $\Phi$ . Most of the existing measures of association involve random vectors  $\mathbf{U} = (\cos \Theta, \sin \Theta)^T$  and  $\mathbf{V} = (\cos \Phi, \sin \Phi)^T$  in the plain. We introduce the following notations

$$\begin{aligned} S_{\Theta\Theta} &= E(\mathbf{U}\mathbf{U}^T) = E \begin{pmatrix} \cos^2 \Theta & \cos \Theta \sin \Theta \\ \sin \Theta \cos \Theta & \sin^2 \Theta \end{pmatrix}, \\ S_{\Theta\Phi} &= E(\mathbf{U}\mathbf{V}^T) = E \begin{pmatrix} \cos \Theta \cos \Phi & \cos \Theta \sin \Phi \\ \sin \Theta \cos \Phi & \sin \Theta \sin \Phi \end{pmatrix}, \\ S_{\Phi\Theta} &= E(\mathbf{V}\mathbf{U}^T) = E \begin{pmatrix} \cos \Phi \cos \Theta & \cos \Phi \sin \Theta \\ \sin \Phi \cos \Theta & \sin \Phi \sin \Theta \end{pmatrix}, \\ S_{\Phi\Phi} &= E(\mathbf{V}\mathbf{V}^T) = E \begin{pmatrix} \cos^2 \Phi & \cos \Phi \sin \Phi \\ \sin \Phi \cos \Phi & \sin^2 \Phi \end{pmatrix}. \end{aligned}$$

#### 3.1 Circular autocorrelation functions

The circular correlation coefficient proposed by Fisher and Lee (1983) is written as

$$\rho_{\text{FL}}(\Theta, \Phi) = \frac{\det(S_{\Theta\Phi})}{\{\det(S_{\Theta\Theta}) \det(S_{\Phi\Phi})\}^{1/2}}.$$

Because of the stationarity, the quantities  $\boldsymbol{\mu} = E(\mathbf{U}_t)$  and  $\Gamma_k = E(\mathbf{U}_{t+k}\mathbf{U}_t^T)$  do not depend on time  $t$ . Then, as proposed in [Holzmann et al. \(2006\)](#), the circular autocorrelation function (CACF) at lag  $k$  is naturally defined by

$$r_k^{(C)} = \rho_{\text{FL}}(\Theta_{t+k}, \Theta_t) = \frac{\det E(\mathbf{U}_k\mathbf{U}_0^T)}{\det E(\mathbf{U}_0\mathbf{U}_0^T)}. \quad (8)$$

Now, we give the CACF of the process (3). Note that  $\Gamma_{-k} = \Gamma_k^T$  and

$$\begin{aligned} \Gamma_0 &= E \left[ \begin{pmatrix} \cos^2 \Theta_0 & \cos \Theta_0 \sin \Theta_0 \\ \sin \Theta_0 \cos \Theta_0 & \sin^2 \Theta_0 \end{pmatrix} \right] = \frac{1}{2} E \left[ \begin{pmatrix} \cos 2\Theta_0 + 1 & \sin 2\Theta_0 \\ \sin 2\Theta_0 & -\cos 2\Theta_0 + 1 \end{pmatrix} \right] \\ &= \frac{1}{2} \begin{pmatrix} \alpha_2^{(f)} + 1 & \beta_2^{(f)} \\ \beta_2^{(f)} & 1 - \alpha_2^{(f)} \end{pmatrix} = \frac{1}{2} I_2, \end{aligned}$$

where  $\alpha_2^{(f)}$  and  $\beta_2^{(f)}$  are the second trigonometric moment of the marginal distribution  $f$  in (1) that is  $E_f[e^{i2\Theta}] = \alpha_2^{(f)} + i\beta_2^{(f)}$ . Since we assume  $f$  is a circular uniform distribution, we have  $\alpha_2^{(f)} = 0$  and  $\beta_2^{(f)} = 0$ . Then,  $\Gamma_k$  can be obtained recursively as follows.

$$\begin{aligned} \Gamma_k &= E(\mathbf{U}_t\mathbf{U}_{t-k}^T) = E[E(\mathbf{U}_t\mathbf{U}_{t-k}^T | \Theta_{t-1:t-p})] \\ &= E[E(\mathbf{U}_t | \Theta_{t-1:t-p})\mathbf{U}_{t-k}^T] = E \left[ \sum_{i=1}^p a_i D_1 Q_i \mathbf{U}_{t-i} \mathbf{U}_{t-k}^T \right] \\ &= \sum_{i=1}^p a_i D_1 Q_i \Gamma_{k-i}. \end{aligned} \quad (9)$$

The following theorem gives the CACF for the  $p$ -th order circular Markov processes. The proof is omitted, since it is obvious from the above discussion.

**Theorem 1.** *Assume that Assumption 1 holds, the lag  $k$  CACF of the process  $\{\Theta_t\}_{t \in \mathbb{Z}}$  given by (8) becomes*

$$r_k^{(C)} = \frac{\det \Gamma_k}{\det \Gamma_0}, \quad (10)$$

where  $\Gamma_k$  are obtained recursively using relation (9) with  $\Gamma_0 = \frac{1}{2} I_2$ .

The sample CACF at lag  $k$  is defined by

$$\hat{r}_k^{(C)} = \frac{\det \hat{\Gamma}_k}{\det \hat{\Gamma}_0},$$

where

$$\hat{\Gamma}_k = \frac{1}{n-k} \sum_{t=k+1}^n \mathbf{U}_t \mathbf{U}_{t-k}^T. \quad (11)$$

The obtained CACF is a natural extension of the result given by [Holzmann et al. \(2006\)](#), where they considered the von Mises distribution for  $g$  and first-order Markov process with order  $p = 1$ . [Abe et al. \(2017\)](#) studied the arbitrary binding density function for  $g$  and

obtained similar CACF as that obtained by [Holzmann et al. \(2006\)](#). The result given in [Theorem 1](#) is the CACF for general  $p$ -th order circular Markov processes on the circle, which is a natural extension of the results given in [Holzmann et al. \(2006\)](#); [Abe et al. \(2017\)](#).

In what follows, we illustrate the CACF for the MTD-AR( $p$ ) models for  $p = 1, 2$ .

**Remark 4** (MTD-AR(1) case). From [\(9\)](#), we have

$$\Gamma_k = D_1 Q_1 \Gamma_{k-1} = (D_1 Q_1)^k \Gamma_0 \quad \text{and} \quad \det \Gamma_k = (q_1 \rho_1^2)^k / 4.$$

Then we observe  $r_k^{(C)} = q_1^k \rho_1^{2k}$ . This is the same result of [Abe et al. \(2017\)](#). If we choose  $g$  as von Mises distribution with location  $\mu_{\text{VM}}$  and concentration  $\kappa_{\text{VM}}$ , then  $r_k^{(C)} = q^k \left( \frac{I_1(\kappa_{\text{VM}})}{I_0(\kappa_{\text{VM}})} \right)^{2k}$ , where  $I_\nu(x)$  is the modified Bessel function of the first kind of order  $\nu$ .

**Remark 5** (MTD-AR(2) case). To solve the general expression for  $\Gamma_k$  by using the recursive expression

$$\Gamma_k = a_1 D_1 Q_1 \Gamma_{k-1} + a_2 D_1 Q_2 \Gamma_{k-2},$$

we observe for  $k = 1$  and  $\Gamma_0 = I_2/2$  that

$$\Gamma_1 = \frac{a_1}{2} D_1 Q_1 I_2 + a_2 D_1 Q_2 \Gamma_{-1}.$$

Recall that  $\Gamma_{-1} = \Gamma_1^T$  and writing  $\Gamma_1 = [\gamma_{1,ij}]_{i,j=1,2}$ , the entries  $\gamma_{1,ij}$  are the solution of the following equations

$$\begin{pmatrix} 1 - a_2 \rho_1 \cos \mu_1 & a_2 \rho_1 q_2 \sin \mu_1 & 0 & 0 \\ 0 & 1 & -a_2 \rho_1 \cos \mu_1 & a_2 \rho_1 q_2 \sin \mu_1 \\ -a_2 \rho_1 \sin \mu_1 & -a_2 \rho_1 q_2 \cos \mu_1 & 1 & 0 \\ 0 & 0 & -a_2 \rho_1 \sin \mu_1 & 1 - a_2 \rho_1 q_2 \cos \mu_1 \end{pmatrix} \begin{pmatrix} \gamma_{1,11} \\ \gamma_{1,12} \\ \gamma_{1,21} \\ \gamma_{1,22} \end{pmatrix} = \frac{a_1 \rho_1}{2} \begin{pmatrix} \cos \mu_1 \\ -q_1 \sin \mu_1 \\ \sin \mu_1 \\ q_1 \cos \mu_1 \end{pmatrix}.$$

Then the circular autocorrelation function can be calculated from relation [\(9\)](#).

Since the expression for the circular autocorrelation function for MTD-AR( $p$ ) becomes complicated, we provide the following assumption on the binding density, which makes the model rather simple and concise.

**Assumption 2.** *The mean direction for the binding density  $g$  is fixed at  $\mu_1 = 0$ .*

This assumption implies the processes  $\cos \Theta_t$  and  $\sin \Theta_t$  are independent of each other as can be convinced from the definition of  $D_1$  whose off-diagonal elements became 0. In addition, this assumption ensures the symmetry of the covariance matrices  $\Gamma_j$  such that  $\Gamma_{-j} = \Gamma_j^T = \Gamma_j$ .

**Remark 6** (MTD-AR(2) case (ii)). Assume that Assumptions 1 and 2 hold. Then, the expression (9) reduces to

$$\Gamma_1 = \begin{pmatrix} 1 - a_2\rho_1 & 0 \\ 0 & 1 - a_2\rho_1q_2 \end{pmatrix}^{-1} \cdot \frac{1}{2} \begin{pmatrix} a_1\rho_1 & 0 \\ 0 & a_1\rho_1q_1 \end{pmatrix}$$

and

$$\det \Gamma_1 = \frac{q_1(a_1\rho_1)^2}{4(1 - a_2\rho_1)(1 - a_2\rho_1q_2)}.$$

Similarly, for  $k = 2$ ,

$$\Gamma_2 = \frac{1}{2} \begin{pmatrix} \left(\frac{(a_1\rho_1)^2}{1 - a_2\rho_1} + a_2\rho_1\right) & 0 \\ 0 & \left(\frac{(q_1a_1\rho_1)^2}{1 - q_2a_2\rho_1} + q_2a_2\rho_1\right) \end{pmatrix}$$

and

$$\det \Gamma_2 = \frac{1}{4} \left( \frac{(a_1\rho_1)^2}{1 - a_2\rho_1} + a_2\rho_1 \right) \left( \frac{(q_1a_1\rho_1)^2}{1 - q_2a_2\rho_1} + q_2a_2\rho_1 \right).$$

Write  $\Gamma_k = [\gamma_{k,ij}]_{i,j=1,2}$ , then we have

$$\det \Gamma_k = \gamma_{k,11}\gamma_{k,22} = (a_1\rho_1\gamma_{k-1,11} + a_2\rho_1\gamma_{k-2,11})(q_1a_1\rho_1\gamma_{k-1,22} + q_2a_2\rho_1\gamma_{k-2,22}).$$

Then the lag  $k$  CACF  $r_k^{(C)}$ s are calculated as follows

$$\begin{aligned} r_1^{(C)} &= \frac{q_1(a_1\rho_1)^2}{(1 - a_2\rho_1)(1 - q_2a_2\rho_1)}, \\ r_2^{(C)} &= \left( \frac{(a_1\rho_1)^2}{1 - a_2\rho_1} + a_2\rho_1 \right) \left( \frac{(q_1a_1\rho_1)^2}{1 - q_2a_2\rho_1} + q_2a_2\rho_1 \right), \\ r_k^{(C)} &= 4(a_1\rho_1\gamma_{k-1,11} + a_2\rho_1\gamma_{k-2,11})(q_1a_1\rho_1\gamma_{k-1,22} + q_2a_2\rho_1\gamma_{k-2,22}) \quad \text{for } k \geq 3. \end{aligned}$$

To evaluate CACF for a general MTD-AR( $p$ ) process, let

$$\phi_1(z) = (1 - a_1\rho_1z - \dots - a_p\rho_1z^p) \tag{12}$$

and

$$\phi_2(z) = (1 - q_1a_1\rho_1z - \dots - q_pa_p\rho_1z^p) \tag{13}$$

be the characteristic polynomials for  $\gamma_{k,11}$  and  $\gamma_{k,22}$ , respectively. We see the CACF  $r_k^{(C)} = 4\gamma_{k,11}\gamma_{k,22}$  is determined by the product of the difference equations for  $k > 0$

$$\phi_1(B)\gamma_{k,11} = 0 \quad \text{and} \quad \phi_2(B)\gamma_{k,22} = 0 \tag{14}$$

where  $B$  denotes the backshift operator. Then, we obtain

$$\phi_1(z)\phi_2(z) = \prod_{i=1}^{m_1} (1 - G_{1,i}z)^{d_{1,i}} \prod_{i=1}^{m_2} (1 - G_{2,i}z)^{d_{2,i}},$$

where  $G_{1,i}^{-1}$  ( $i = 1, 2, \dots, m_1$ ) and  $G_{2,i}^{-1}$  ( $i = 1, 2, \dots, m_2$ ) are the roots of the polynomials  $\phi_1(z) = 0$  and  $\phi_2(z) = 0$ , respectively, and  $\sum_{i=1}^{m_j} d_{j,i} = p$  for  $j = 1, 2$ . Then the CACF is given by the following result.

**Theorem 2.** Under Assumptions 1 and 2 holds. The lag  $k$  CACF for MTD-AR( $p$ ) process is given by

$$r_k^{(C)} = \left( \sum_{i=1}^{m_1} G_{1,i}^k \sum_{j=0}^{d_{1,i}-1} A_{1,ij} k^j \right) \left( \sum_{i=1}^{m_2} G_{2,i}^k \sum_{j=0}^{d_{2,i}-1} A_{2,ij} k^j \right).$$

If  $d_{j,i} = 1$  for all  $i = 1, \dots, p$  and  $j = 1, 2$ ,  $G_{1,i}^{-1}$  and  $G_{2,i}^{-1}$  are all distinct and the CACF reduces to

$$r_k^{(C)} = \left( \sum_{i=1}^p A_{1,i} G_{1,i}^k \right) \left( \sum_{i=1}^p A_{2,i} G_{2,i}^k \right), \quad k > 0,$$

where  $A_{1,i}$  and  $A_{2,i}$  are the constants obtained recursively using (9) for  $k = 1, 2, \dots, p$ .

### 3.2 Circular partial autocorrelation functions

We have investigated second-order stationarity and CACF of the MTD-AR( $p$ ) models so far. Here we will provide a CPACF for MTD-AR( $p$ ) models. The process considered here is the bivariate process  $\mathbf{U}_t = (\cos \Theta_t, \sin \Theta_t)^T$  defined in Section 3.1. Recall that the expressions of the forward and backward innovations of  $\mathbf{U}_t$  are different, the simple expression of the partial autocorrelation function (PACF) is difficult to obtain, see Morf et al. (1978) and Degerine (1990), for PACF for multivariate time series.

Below we define the CPACF, following the manner of Degerine (1990). The best linear predictor  $\widehat{\mathbf{U}}_{t,s}$  is the projection onto the  $s$  past valued linear space. Write the  $s$ -th order forward innovation  $\boldsymbol{\varepsilon}_t$  as

$$\boldsymbol{\varepsilon}_{t,s} = \mathbf{U}_t - \widehat{\mathbf{U}}_{t,s} = \mathbf{U}_t - \sum_{j=1}^s \Xi_j \mathbf{U}_{t-j},$$

The solution of  $\Xi_j$ ,  $j = 1, \dots, s$  is obtained by the following linear equations

$$\begin{bmatrix} \Xi_1 & \Xi_2 & \cdots & \Xi_s \end{bmatrix} \begin{bmatrix} \Gamma_0 & \Gamma_1 & \cdots & \Gamma_{s-1} \\ \Gamma_{-1} & \Gamma_0 & \cdots & \Gamma_{s-2} \\ \vdots & \vdots & \ddots & \vdots \\ \Gamma_{1-s} & \Gamma_{2-s} & \cdots & \Gamma_0 \end{bmatrix} = \begin{bmatrix} \Gamma_1 & \Gamma_2 & \cdots & \Gamma_s \end{bmatrix}. \quad (15)$$

Similarly, the  $n$ -th order backward innovation  $\boldsymbol{\varepsilon}_{t,s}^*$  can be defined as

$$\boldsymbol{\varepsilon}_{t,s}^* = \mathbf{U}_t - \widehat{\mathbf{U}}_{t,s}^* = \mathbf{U}_t - \sum_{j=1}^s \Xi_j^* \mathbf{U}_{t+j}.$$

The solution of  $\Xi_j^*$ ,  $j = 1, \dots, s$  is obtained by following linear equations

$$\begin{bmatrix} \Xi_1^* & \Xi_2^* & \cdots & \Xi_s^* \end{bmatrix} \begin{bmatrix} \Gamma_0 & \Gamma_{-1} & \cdots & \Gamma_{1-s} \\ \Gamma_1 & \Gamma_0 & \cdots & \Gamma_{2-s} \\ \vdots & \vdots & \ddots & \vdots \\ \Gamma_{s-1} & \Gamma_{s-2} & \cdots & \Gamma_0 \end{bmatrix} = \begin{bmatrix} \Gamma_{-1} & \Gamma_{-2} & \cdots & \Gamma_{-s} \end{bmatrix}. \quad (16)$$

Then the partial autocovariance matrix of the process  $U_t$  is defined by

$$\Psi_s = E[\boldsymbol{\varepsilon}_{t,s-1} \boldsymbol{\varepsilon}_{t-s,s-1}^*{}^T].$$

Similar to the definition of the CACF, we propose a CPACF as

$$\psi_s^{(C)} = \frac{\det(\Psi_s)}{\{\det E(\boldsymbol{\varepsilon}_{t,s-1} \boldsymbol{\varepsilon}_{t,s-1}^T) \det E(\boldsymbol{\varepsilon}_{t,s-1}^* \boldsymbol{\varepsilon}_{t,s-1}^T)\}^{1/2}}. \quad (17)$$

The general expressions for the CPACF are complicated forms, however, we can obtain rather simple expressions under Assumption 2. This is because the forward and backward innovations are equivalent due to the symmetry of the matrices  $\Gamma_k$ . The CPACF is stated as in the following theorem.

**Theorem 3.** *Assume that Assumptions 1 and 2 hold. Then the lag  $s$  PCACF of the MTD-AR( $p$ ) process  $\{\Theta_t\}_{t \in \mathbb{Z}}$  given by (17) can be obtained by solving*

$$\psi_s^{(C)} = \frac{\begin{vmatrix} \Gamma_0 & \Gamma_1 & \cdots & \Gamma_{s-2} & \Gamma_1 \\ \Gamma_1 & \Gamma_0 & \cdots & \Gamma_{s-3} & \Gamma_2 \\ \vdots & \vdots & & \vdots & \vdots \\ \Gamma_{s-1} & \Gamma_{s-2} & \cdots & \Gamma_1 & \Gamma_s \end{vmatrix}}{\begin{vmatrix} \Gamma_0 & \Gamma_1 & \cdots & \Gamma_{s-2} & \Gamma_{s-1} \\ \Gamma_1 & \Gamma_0 & \cdots & \Gamma_{s-3} & \Gamma_{s-2} \\ \vdots & \vdots & & \vdots & \vdots \\ \Gamma_{s-1} & \Gamma_{s-2} & \cdots & \Gamma_1 & \Gamma_0 \end{vmatrix}}. \quad (18)$$

The sample CPACF is defined by

$$\widehat{\psi}_k^{(C)} = \frac{\begin{vmatrix} \widehat{\Gamma}_0 & \widehat{\Gamma}_1 & \cdots & \widehat{\Gamma}_{k-2} & \widehat{\Gamma}_1 \\ \widehat{\Gamma}_1^T & \widehat{\Gamma}_0 & \cdots & \widehat{\Gamma}_{k-3} & \widehat{\Gamma}_2 \\ \vdots & \vdots & & \vdots & \vdots \\ \widehat{\Gamma}_{k-1}^T & \widehat{\Gamma}_{k-2}^T & \cdots & \widehat{\Gamma}_1^T & \widehat{\Gamma}_k \end{vmatrix}}{\begin{vmatrix} \widehat{\Gamma}_0 & \widehat{\Gamma}_1 & \cdots & \widehat{\Gamma}_{k-2} & \widehat{\Gamma}_{k-1} \\ \widehat{\Gamma}_1^T & \widehat{\Gamma}_0 & \cdots & \widehat{\Gamma}_{k-3} & \widehat{\Gamma}_{k-2} \\ \vdots & \vdots & & \vdots & \vdots \\ \widehat{\Gamma}_{k-1}^T & \widehat{\Gamma}_{k-2}^T & \cdots & \widehat{\Gamma}_1^T & \widehat{\Gamma}_0 \end{vmatrix}}.$$

where  $\widehat{\Gamma}_k$  is defined by (11). It must be noted that the sample covariance matrix at lag  $k$  of  $\widehat{\Gamma}_k$  is not a symmetric matrix.

**Remark 7** (MTD-AR(2) case). Here we provide the CPACF of the MTD-AR(2) process as follows. For  $k = 1$ , we observe

$$\Gamma_1 = \begin{pmatrix} 1 - a_2 \rho_1 & 0 \\ 0 & 1 - a_2 \rho_1 q_2 \end{pmatrix}^{-1} \cdot \frac{1}{2} \begin{pmatrix} a_1 \rho_1 & 0 \\ 0 & a_1 \rho_1 q_1 \end{pmatrix}$$

and

$$\det \Gamma_1 = \frac{q_1 (a_1 \rho_1)^2}{4(1 - a_2 \rho_1)(1 - a_2 \rho_1 q_2)}.$$

Then,  $\psi_1^{(C)}$  becomes

$$\begin{aligned} \psi_1^{(C)} &= \frac{q_1 (a_1 \rho_1)^2}{(1 - a_2 \rho_1)(1 - a_2 \rho_1 q_2)} = \frac{a_1 \rho_1}{1 - a_2 \rho_1} \cdot \frac{q_1 a_1 \rho_1}{1 - a_2 \rho_1 q_2} \\ &=: \rho_c(1) \cdot \rho_s(1), \end{aligned}$$

where  $\rho_c(1)$  and  $\rho_s(1)$  are the lag 1 partial autocorrelation function of the  $\cos \Theta_t$  and  $\sin \Theta_t$  processes whose characteristic equations are defined by equations (12) and (13), respectively, with order  $p = 2$ . Similarly, for  $k = 2$ , we have

$$\psi_2^{(C)} = \frac{\begin{vmatrix} \Gamma_0 & \Gamma_1 \\ \Gamma_1 & \Gamma_2 \end{vmatrix}}{\begin{vmatrix} \Gamma_0 & \Gamma_1 \\ \Gamma_1 & \Gamma_0 \end{vmatrix}}.$$

After some calculations, the denominator becomes

$$\begin{vmatrix} \Gamma_0 & \Gamma_1 \\ \Gamma_1 & \Gamma_0 \end{vmatrix} = \frac{1}{4}(1 - \rho_c(1)^2) \times \frac{1}{4}(1 - \rho_s(1)^2).$$

As for the numerator, we obtain

$$\begin{vmatrix} \Gamma_0 & \Gamma_1 \\ \Gamma_1 & \Gamma_2 \end{vmatrix} = \frac{1}{4}(\rho_c(2) - \rho_c(1)^2) \times \frac{1}{4}(\rho_s(2) - \rho_s(1)^2),$$

where  $\rho_c(2) = \frac{(a_1\rho_1)^2}{1-a_1\rho_1} + a_2\rho_1$  and  $\rho_s(2) = \frac{(q_1a_1\rho_1)^2}{1-q_2a_1\rho_1} + q_2a_2\rho_1$  are the lag 2 partial autocorrelation function for the AR(2) of the  $\cos \Theta_t$  and  $\sin \Theta_t$  processes. Then, we get

$$\psi_2^{(C)} = \frac{\rho_c(2) - \rho_c(1)^2}{1 - \rho_c(1)^2} \times \frac{\rho_s(2) - \rho_s(1)^2}{1 - \rho_s(1)^2}.$$

This indicates that the circular partial autocorrelation function at lag 2 is the product of the partial autocorrelation function at lag 2 for the linear AR(2) process of  $\cos \Theta_t$  and  $\sin \Theta_t$ . Finally, for  $k = 3$ , we have

$$\psi_3^{(C)} = \frac{\begin{vmatrix} \Gamma_0 & \Gamma_1 & \Gamma_1 \\ \Gamma_1 & \Gamma_0 & \Gamma_2 \\ \Gamma_2 & \Gamma_1 & \Gamma_3 \end{vmatrix}}{\begin{vmatrix} \Gamma_0 & \Gamma_1 & \Gamma_2 \\ \Gamma_1 & \Gamma_0 & \Gamma_1 \\ \Gamma_2 & \Gamma_1 & \Gamma_0 \end{vmatrix}}.$$

The numerator becomes

$$(1/2)^3\{(\rho_c(3) - \rho_c(1)\rho_c(2)) - \rho_c(1)^2(\rho_c(3) - \rho_c(1)) + \rho_c(2)\rho_c(1)(\rho_c(2) - 1)\} \\ \times (1/2)^3\{(\rho_s(3) - \rho_s(1)\rho_s(2)) - \rho_s(1)^2(\rho_s(3) - \rho_s(1)) + \rho_s(2)\rho_s(1)(\rho_s(2) - 1)\},$$

where  $\rho_c(3) = a_1\rho_1\rho_c(2) + a_2\rho_1\rho_c(1)$  and  $\rho_s(3) = q_1a_1\rho_1\rho_s(2) + q_2a_2\rho_1\rho_s(1)$  are the partial autocorrelation function for the AR(2) of  $\cos \Theta_t$  and  $\sin \Theta_t$  processes, respectively. Since we have  $\rho_c(3) = \rho_s(3) = 0$ , the CPACF at lag 3 becomes 0. The analogous calculation yields that  $\psi_k^{(C)} = 0$  for  $k \geq 4$ .

### 3.3 Spectral density function of the higher-order circular time series

The quantity  $\det \Gamma_k$  can be considered as the circular autocovariance function as explained in Abe et al. (2017). Hence, by using the Fourier series expansion of  $\det \Gamma_k$ , we can obtain

the spectral density for the circular stationary process. We say  $\det \Gamma_k$  in (10) as the valid circular autocovariance function and the corresponding spectral density is expressed as

$$f_{\Theta}(\omega) = \frac{1}{2\pi} \sum_{k=-\infty}^{\infty} e^{-i\omega k} \det \Gamma_k = \frac{1}{2\pi} \sum_{k=-\infty}^{\infty} e^{-i\omega k} \begin{vmatrix} \gamma_{k,11} & \gamma_{k,12} \\ \gamma_{k,21} & \gamma_{k,22} \end{vmatrix}.$$

Then we obtain the following result.

**Theorem 4.** *Assume that Assumptions 1 and 2 hold. Let the AR characteristic polynomials  $\phi_1(z)$  and  $\phi_2(z)$  of the processes  $\cos \Theta_t$  and  $\sin \Theta_t$  are defined by (12) and (13), respectively. Then, the spectral density function for MTD-AR( $p$ ) process defined by (3) is given by*

$$f_{\Theta}(\omega) = \int_{-\pi}^{\pi} f_{X_1}(\lambda) f_{X_2}(\omega - \lambda) d\lambda,$$

where  $f_{X_1}(\omega)$  and  $f_{X_2}(\omega)$  are the spectral density functions of the process  $\cos \Theta_t$  and  $\sin \Theta_t$ , which are given by

$$f_{X_1}(\omega) = \frac{1 - 2\rho_1 \sum_{i=1}^p a_i \gamma_{i,11}}{4\pi |\phi_1(e^{-i\omega})|^2} \quad \text{and} \quad f_{X_2}(\omega) = \frac{1 - 2\rho_1 \sum_{i=1}^p q_i a_i \gamma_{i,22}}{4\pi |\phi_2(e^{-i\omega})|^2},$$

respectively.

Practically, the spectral density is calculated as follows.

$$\begin{aligned} f_{\Theta}(\omega) &= \int_{-\pi}^{\pi} f_{X_1}(\lambda) f_{X_2}(\omega - \lambda) d\lambda \\ &= \frac{(1 - 2\rho_1 \sum_{i=1}^p a_i \gamma_{i,11})(1 - 2\rho_1 \sum_{i=1}^p q_i a_i \gamma_{i,22})}{16\pi^2} \\ &\quad \times \int_{-\pi}^{\pi} \frac{d\lambda}{\prod_{i=1}^{m_1} (1 - G_{1,i} e^{-i\lambda})^{d_{1,i}} (1 - G_{1,i}^* e^{i\lambda})^{d_{1,i}} \prod_{i=1}^{m_2} (1 - G_{2,i} e^{-i(\omega-\lambda)})^{d_{2,i}} (1 - G_{2,i}^* e^{i(\omega-\lambda)})^{d_{2,i}}}. \end{aligned}$$

Set  $z = e^{i\lambda}$ , then we have  $d\lambda = dz/(iz)$  and the above integral becomes

$$\begin{aligned} &\frac{1}{i} \int_C \frac{dz}{z \prod_{i=1}^{m_1} (1 - \frac{G_{1,i}}{z})^{d_{1,i}} (1 - G_{1,i}^* z)^{d_{1,i}} \prod_{i=1}^{m_2} (1 - G_{2,i} e^{-i\omega} z)^{d_{2,i}} (1 - \frac{G_{2,i}^* e^{i\omega}}{z})^{d_{2,i}}} \\ &= \frac{1}{i} \int_C \frac{1}{z \prod_{i=1}^{m_1} (\frac{1}{z})^{d_{1,i}} (z - G_{1,i})^{d_{1,i}} (-G_{1,i}^*)^{d_{1,i}} (z - \frac{1}{G_{1,i}^*})^{d_{1,i}}} \\ &\quad \times \frac{1}{\prod_{i=1}^{m_2} (-G_{2,i} e^{-i\omega})^{d_{2,i}} (z - \frac{1}{G_{2,i} e^{-i\omega}})^{d_{2,i}} (\frac{1}{z})^{d_{2,i}} (z - G_{2,i}^* e^{i\omega})^{d_{2,i}}} dz \\ &= \frac{1}{i \prod_{i=1}^{m_1} (-G_{1,i}^*)^{d_{1,i}} \prod_{i=1}^{m_2} (-G_{2,i} e^{-i\omega})^{d_{2,i}}} \\ &\quad \times \int_C \frac{z^{2p-1}}{\prod_{i=1}^{m_1} (z - G_{1,i})^{d_{1,i}} (z - \frac{1}{G_{1,i}^*})^{d_{1,i}} \prod_{i=1}^{m_2} (z - \frac{1}{G_{2,i} e^{-i\omega}})^{d_{2,i}} (z - G_{2,i}^* e^{i\omega})^{d_{2,i}}} dz, \quad (19) \end{aligned}$$

where  $C = \{z \in \mathbb{C} : |z| = 1\}$ . The integrand in (19) has poles of order  $d_{1,i}$  at  $z = G_{1,i}$  ( $i = 1, 2, \dots, m_1$ ), order  $d_{2,i}$  at  $z = G_{2,i}^* e^{i\omega}$  ( $i = 1, 2, \dots, m_2$ ). From the residue theorem, the integral is equal to  $(2\pi i)$  times of the sum of the all residues. Therefore, the spectral density of  $\Theta_t$  is

$$\frac{(1 - 2\rho_1 \sum_{i=1}^p a_i \gamma_{i,11})(1 - 2\rho_1 \sum_{i=1}^p q_i a_i \gamma_{i,22})}{8\pi \prod_{i=1}^{m_1} (-G_{1,i}^*)^{d_{1,i}} \prod_{i=1}^{m_2} (-G_{2,i} e^{-i\omega})^{d_{2,i}}} \left\{ \sum_{i=1}^{m_1} \text{Res}(G_{1,i}) + \sum_{i=1}^{m_2} \text{Res}(G_{2,i}^* e^{i\omega}) \right\} \quad (20)$$

The residue at  $z = G_{1,i}$  is

$$\begin{aligned} \text{Res}(G_{1,i}) &= \frac{1}{(d_{1,i} - 1)!} \left( \frac{d}{dz} \right)^{d_{1,i} - 1} \\ &\times \frac{z^{2p-1}}{\prod_{j=1, j \neq i}^{m_1} (z - G_{1,j})^{d_{1,j}} \prod_{j=1}^{m_1} \left( z - \frac{1}{G_{1,j}^*} \right)^{d_{1,j}} \prod_{j=1}^{m_2} \left( z - \frac{1}{G_{2,j} e^{-i\omega}} \right)^{d_{2,j}} (z - G_{2,j}^* e^{i\omega})^{d_{2,j}}} \Big|_{z=G_{1,i}} \end{aligned} \quad (21)$$

To derive the  $(d_{1,i} - 1)$ th derivative in (21), let

$$v(z) = \frac{z^{2p-1}}{\prod_{j=1, j \neq i}^{m_1} (z - G_{1,j})^{d_{1,j}} \prod_{j=1}^{m_1} \left( z - \frac{1}{G_{1,j}^*} \right)^{d_{1,j}} \prod_{j=1}^{m_2} \left( z - \frac{1}{G_{2,j} e^{-i\omega}} \right)^{d_{2,j}} (z - G_{2,j}^* e^{i\omega})^{d_{2,j}}}$$

By taking the logarithm of both sides, we have

$$\begin{aligned} \ln v(z) &= (2p - 1) \ln z - \sum_{j=1, j \neq i}^{m_1} d_{1,j} \ln(z - G_{1,j}) - \sum_{j=1}^{m_1} d_{1,j} \ln\left(z - \frac{1}{G_{1,j}^*}\right) \\ &\quad - \sum_{j=1}^{m_2} d_{2,j} \ln\left(z - \frac{1}{G_{2,j} e^{-i\omega}}\right) - \sum_{j=1}^{m_2} d_{2,j} \ln(z - G_{2,j}^* e^{i\omega}). \end{aligned}$$

Differentiating both sides leads to

$$\frac{\frac{d}{dz} v(z)}{v(z)} = \frac{2p-1}{z} - \sum_{j=1, j \neq i}^{m_1} \frac{d_{1,j}}{z - G_{1,j}} - \sum_{j=1}^{m_1} \frac{d_{1,j}}{z - \frac{1}{G_{1,j}^*}} - \sum_{j=1}^{m_2} \frac{d_{2,j}}{z - \frac{1}{G_{2,j} e^{-i\omega}}} - \sum_{j=1}^{m_2} \frac{d_{2,j}}{z - G_{2,j}^* e^{i\omega}}. \quad (22)$$

Denote the right hand side of (22) by  $w(z)$ . Then, first derivative of  $v(z)$  is

$$\frac{d}{dz} v(z) = v(z) w(z).$$

The  $n$ th order derivative of  $v(z)$  at  $z = G_{1,i}$  is

$$\frac{d^n}{dz^n} v(z) \Big|_{z=G_{1,i}} = \sum_{k=0}^{n-1} \binom{n-1}{k} \frac{d^{n-1-k}}{dz^{n-1-k}} v(z) \Big|_{z=G_{1,i}} \cdot \frac{d^k}{dz^k} w(z) \Big|_{z=G_{1,i}}. \quad (23)$$

The  $k$ th order derivative of  $w(z)$  at  $z = G_{1,i}$  is given by

$$\begin{aligned} \frac{d^k}{dz^k} w(z) \Big|_{z=G_{1,i}} &= (-1)^k k! \left[ (2p-1) G_{1,i}^{-(k+1)} - \sum_{j=1, j \neq i}^{m_1} d_{1,j} (G_{1,i} - G_{1,j})^{-(k+1)} \right. \\ &\quad \left. - \sum_{j=1}^{m_1} d_{1,j} \left( G_{1,i} - \frac{1}{G_{1,j}^*} \right)^{-(k+1)} - \sum_{j=1}^{m_2} d_{2,j} \left( G_{1,i} - \frac{1}{G_{2,j} e^{-i\omega}} \right)^{-(k+1)} - \sum_{j=1}^{m_2} d_{2,j} (G_{1,i} - G_{2,j}^* e^{i\omega})^{-(k+1)} \right] \end{aligned}$$

and we can recursively calculate the  $n$ th derivative in (23). Calculation of the residue at  $z = G_{2,i}^* e^{i\omega}$  is similar.

**Remark 8** (MTD-AR(1) case). Consider the case that the transition density in (3) is  $g(\theta_t - q_1 \theta_{t-1})$ . Set the mean resultant length and mean resultant direction of  $g$  are  $\rho_1$  and

0, respectively. Then, we have  $2\gamma_{1,11} = G_{1,1} = \rho_1$  and  $2\gamma_{1,22} = G_{2,1} = q_1\rho_1$ . By (20), the spectral density function is

$$f_{\Theta}(\omega) = \frac{(1 - \rho_1^2)^2}{8\pi q_1 \rho_1^2 e^{-i\omega}} \{ \text{Res}(\rho_1) + \text{Res}(q_1 \rho_1 e^{i\omega}) \}.$$

Here,

$$\text{Res}(\rho_1) = \frac{\rho_1}{(\rho_1 - \frac{1}{\rho_1})(\rho_1 - \frac{1}{q_1 \rho_1 e^{-i\omega}})(\rho_1 - q_1 \rho_1 e^{i\omega})} = \frac{q_1 \rho_1^2 e^{-i\omega}}{(1 - \rho_1^2)(1 - q_1 \rho_1^2 e^{-i\omega})(1 - q_1 e^{i\omega})}$$

and

$$\begin{aligned} \text{Res}(q_1 \rho_1 e^{i\omega}) &= \frac{q_1 \rho_1 e^{i\omega}}{(q_1 \rho_1 e^{i\omega} - \rho_1)(q_1 \rho_1 e^{i\omega} - \frac{1}{\rho_1})(q_1 \rho_1 e^{i\omega} - \frac{1}{q_1 \rho_1 e^{-i\omega}})} \\ &= \frac{-\rho_1^2}{(1 - \rho_1^2)(1 - q_1 \rho_1^2 e^{i\omega})(1 - q_1 e^{i\omega})}. \end{aligned}$$

Finally, we have

$$f_{\Theta}(\omega) = \frac{(1 - \rho_1^2)(1 + \rho_1^2)}{8\pi |1 - q_1 \rho_1^2 e^{i\omega}|^2}.$$

## 4 Maximum Likelihood Estimation

For the MTD models studied by, for example, [Le et al. \(1996\)](#); [Raftery and Tavaré \(1994\)](#), the maximum likelihood estimation with EM algorithm is a standard estimation method since it works well for a very large and highly nonlinear class of MTD models ([Berchtold and Raftery, 2002](#)). However, the estimates of EM algorithms tend to have a local optimum solution rather than a global one. In addition, the iterative procedures need a large computational time to converge. This section provides the maximum likelihood estimation methods for unknown model parameters without implementing EM algorithms. Let the parameter vector be  $\boldsymbol{\eta} = (a_1, \dots, a_{p-1}, \rho)^T$  and  $\boldsymbol{q} = (q_1, \dots, q_p)^T$  for the MTD model in (3). The parameter space for  $(a_1, \dots, a_{p-1})$  is denoted by  $\mathbf{A}$  which is defined by

$$\mathbf{A} = \left\{ (a_1, \dots, a_{p-1}) \mid 0 \leq a_i \leq 1 - \delta_{A_1}, \sum_{i=1}^{p-1} a_i \leq 1 - \delta_{A_2} \right\},$$

for some  $\delta_{A_1} > 0$  and  $\delta_{A_2} > 0$ . The parameter space of a concentration parameter of a binding density  $g$  is denoted by  $R_{\rho} = (0, \bar{R}_{\rho}]$ . For the wrapped Cauchy distributions, we set  $\rho \in [\delta_{\rho}, 1 - \delta_{\rho}]$ , and for the von Mises distribution, we set  $\rho = \kappa$  and  $\kappa \in [\delta_{\kappa}, \bar{R}_{\kappa}]$ , where  $\delta_{\rho}$  and  $\delta_{\kappa}$  are small constants and  $0 < \bar{R}_{\kappa} < \infty$ . Then, we define a parameter space of  $\boldsymbol{\eta}$  as  $\mathbf{H} = \mathbf{A} \times R_{\rho}$ . Since the direction of the dependency parameter vector  $\boldsymbol{q}$  is discrete values, the parameter spaces for  $\boldsymbol{q}$  is denoted by  $\mathbf{Q}$  which is defined by

$$\mathbf{Q} = \{(q_1, q_2, \dots, q_p) \mid q_i \in \{1, -1\}, i = 1, \dots, p\}.$$

The log-likelihood function of the model becomes:

$$\ell_n(\boldsymbol{\eta}, \mathbf{q}) = \sum_{t=p+1}^n \ln \left( \sum_{i=1}^p a_i g(\theta_t - q_i \theta_{t-i}; \rho) \right).$$

The MLE of  $\hat{\boldsymbol{\eta}}_n$  and  $\hat{\mathbf{q}}_n$  are obtained by maximizing the log-likelihood function over the parameter spaces  $\mathbf{H}$  and  $\mathbf{Q}$  as follows:

$$(\hat{\boldsymbol{\eta}}_n, \hat{\mathbf{q}}_n) = \operatorname{argmax}_{\boldsymbol{\eta} \in \mathbf{H}, \mathbf{q} \in \mathbf{Q}} \ell_n(\boldsymbol{\eta}, \mathbf{q}).$$

We do not assume that the true binding density  $g$  and true AR order  $p$  belong to the set of distributions of a fitted model. Hence, we call the estimator defined above a quasi-likelihood estimator under the misspecified model. Hereafter, we assume that the direction of the dependency parameter vector  $\mathbf{q}$  is prespecified for simplicity which we denote by  $\mathbf{q}_0 = (q_{10}, \dots, q_{p0})$ . In addition, the autoregressive order  $p$  is also prespecified. To derive asymptotic properties of  $\hat{\boldsymbol{\eta}}_n$  with known  $\mathbf{q}_0$ , we denote the MLE of  $\boldsymbol{\eta}$  as follows

$$\hat{\boldsymbol{\eta}}_n = \operatorname{argmax}_{\boldsymbol{\eta} \in \mathbf{H}} \ell_n(\boldsymbol{\eta}, \mathbf{q}_0).$$

Denote  $\boldsymbol{\eta}_0$  by

$$\boldsymbol{\eta}_0 = \operatorname{argmax}_{\boldsymbol{\eta} \in \mathbf{H}} E \left[ \ln \left( \sum_{i=1}^p a_i g(\Theta_t - q_{i0} \Theta_{t-i}; \rho) \right) \right].$$

We assume the following condition.

**Assumption 3.** (a)  $\mathbf{H}$  is compact, and the  $\boldsymbol{\eta}_0$  belongs to  $\mathbf{H}$ .

(b) The binding density  $g(\cdot)$  is continuous. In addition,  $g(\cdot)$  satisfies

$$\sup_{\rho \in R_\rho} g(\theta; \rho) < \overline{M} \quad \text{and} \quad \inf_{\rho \in R_\rho} g(\theta; \rho) > \underline{M}$$

for some constants  $\overline{M} > 0$  and  $\underline{M} > 0$ , for any  $\theta \in [-\pi, \pi)$ .

(c) The first two derivatives of the binding density  $g(\cdot)$  with respect to parameters  $\rho$  are continuous and bounded for all  $\theta$  and  $\rho \in R_\rho$ .

(d) The Fisher information matrix

$$\mathbf{I}(\boldsymbol{\eta}_0) := -E_{\boldsymbol{\eta}_0} \left[ (\partial^2 / \partial \boldsymbol{\eta} \partial \boldsymbol{\eta}^T) \ln \left( \sum_{i=1}^p a_i g(\Theta_t - q_{i0} \Theta_{t-i}; \rho) \right) \right] \text{ is non-singular.}$$

(e) The family  $\{\sum_{i=1}^p a_i g(\Theta_t - q_{i0} \Theta_{t-i}; \rho)\}$  is identifiable, that implies for parameters

$$\boldsymbol{\eta}_1 = (a_{1,1}, \dots, a_{p-1,1}, \rho_1) \neq (a_{1,2}, \dots, a_{p-1,2}, \rho_2) = \boldsymbol{\eta}_2, \text{ we observe } \{\sum_{i=1}^p a_{i,1} g(\Theta_t - q_{i0} \Theta_{t-i}; \rho_1)\} \neq \{\sum_{i=1}^p a_{i,2} g(\Theta_t - q_{i0} \Theta_{t-i}; \rho_2)\}.$$

Assumptions 3(b) and (c) ensure that the Markov kernel function  $\sum_{i=1}^p a_i g(\Theta_t - q_{i0} \Theta_{t-i}; \rho)$  is continuous and its logarithm is bounded for all  $\boldsymbol{\eta}$ . Examples of binding density functions include well-known symmetric circular densities, such as von Mises and wrapped Cauchy

distributions with location  $\mu = 0$ . Since we assume that  $\inf_{\rho \in R_\rho} g(\theta; \rho) > \underline{M}$  in Assumption 3(b), this guarantees the integrability condition  $E_{\eta_0} \{\ln(\sum_{i=1}^p a_i g(\Theta_t - q_{i0} \Theta_{t-i}; \rho))\} > -\infty$ .

We obtain the following consistency and asymptotic normality properties for the MLE.

**Theorem 5.** (*Consistency*) Let  $\{\hat{\boldsymbol{\eta}}_n\}$  be a sequence of MLE and Assumptions 1–3 hold, then we have as  $n \rightarrow \infty$ ,

$$\hat{\boldsymbol{\eta}}_n \xrightarrow{a.s.} \boldsymbol{\eta}_0.$$

To obtain the limiting distribution of  $\hat{\boldsymbol{\eta}}_n$ , we assume the following assumption instead of Assumption 3(a).

**Assumption 3 (a')**  $\mathbf{H}$  is convex and compact, and the  $\boldsymbol{\eta}_0$  belong to the interior of  $\mathbf{H}$ .

The following result gives the limiting distribution of  $\hat{\boldsymbol{\eta}}_n$ .

**Theorem 6.** (*Asymptotic normality*) Under Assumptions 1, 2, 3(a') and 3(b)–(e), we have

$$\sqrt{n}(\hat{\boldsymbol{\eta}}_n - \boldsymbol{\eta}_0) \xrightarrow{d} N(\mathbf{0}, I(\boldsymbol{\eta}_0)^{-1} \mathbf{J}(\boldsymbol{\eta}_0) I(\boldsymbol{\eta}_0)^{-1}),$$

where  $I(\boldsymbol{\eta}_0)$  is defined by Assumption 3(d) and  $\mathbf{J}(\boldsymbol{\eta}_0)$  is defined by

$$\mathbf{J}(\boldsymbol{\eta}_0) = E_{\eta_0} \left[ \left( \frac{\partial}{\partial \boldsymbol{\eta}} \ell_n(\boldsymbol{\eta}, \mathbf{q}_0) \right) \left( \frac{\partial}{\partial \boldsymbol{\eta}} \ell_n(\boldsymbol{\eta}, \mathbf{q}_0) \right)^T \right].$$

For a misspecified model, the MLE strongly converges to the parameter vector that minimizes the Kullback-Leibler divergence between the true model and the postulated likelihood functions. If we consider a well-specified model, the generalized information matrix equality holds such that  $\mathbf{I}(\boldsymbol{\eta}_0) = \mathbf{J}(\boldsymbol{\eta}_0)$ , which leads the asymptotic distribution of the MLE as follows

$$\sqrt{n}(\hat{\boldsymbol{\eta}}_n - \boldsymbol{\eta}_0) \xrightarrow{d} N(\mathbf{0}, \mathbf{I}(\boldsymbol{\eta}_0)^{-1}).$$

The MLE of the direction of dependency parameters  $\hat{\mathbf{q}}_n$  is obtained by following procedures. Let the  $j$ -th elements of the parameter space  $\mathbf{Q}$  is denoted by  $\mathbf{q}_j$  ( $j = 1, \dots, 2^p$ ), then  $\hat{\mathbf{q}}_n$  is defined by

$$\hat{\mathbf{q}}_n = \operatorname{argmax}_{\mathbf{q}_j \in \mathbf{Q}} \ell_n(\hat{\boldsymbol{\eta}}_n(\mathbf{q}_j), \mathbf{q}_j),$$

where  $\hat{\boldsymbol{\eta}}_n(\mathbf{q}_j)$  is the MLE of  $\boldsymbol{\eta}$  given  $\mathbf{q}_j$ , and the corresponding MLE based on  $\hat{\boldsymbol{\eta}}_n$  is denoted by  $\hat{\boldsymbol{\eta}}_n(\hat{\mathbf{q}}_n)$ .

The unknown order  $p$  and the direction of dependency parameter  $\mathbf{q}$  are selected by using well-known information criteria, Akaike Information Criteria (AIC) and Bayesian Information Criteria (BIC). The parameters of MTD-AR( $p$ ) models consist the mixing weights and the concentration of the binding density, hence, the number of parameters reduces to  $p$ . The definitions of the AIC and BIC are as follows:

$$\text{AIC} = -2\ell_n(\hat{\boldsymbol{\eta}}_n(\hat{\mathbf{q}}_n), \hat{\mathbf{q}}_n) + 2p$$

and

$$\text{BIC} = -2\ell_n(\hat{\boldsymbol{\eta}}_n(\hat{\mathbf{q}}_n), \hat{\mathbf{q}}_n) + p \log n.$$

## 5 Monte Carlo Simulations and Numerical Examples

In this section, we briefly illustrate a numerical example of the statistical properties provided in the previous sections. First, we plot the CACF of the MTD-AR(2) processes. The mixing weight parameter  $\mathbf{a}$  is set as  $(a_1, a_2) = (0.3, 0.7)$ , and the binding density  $g$  is chosen as a wrapped Cauchy distribution with concentration parameter  $\rho = 0.9$ . The direction of the effects of the lagged variables is controlled by the parameter vector  $\mathbf{q} = (q_1, q_2)$ , which is set as  $(q_1, q_2) \in \{(1, 1), (1, -1), (-1, 1), (-1, -1)\}$ . The panels (a) through (d) in Figure 1 show the theoretical CACF given in (17) for four combinations of the signs in the parameters  $(q_1, q_2)$ . We can confirm that from panel (a), the positively autocorrelated time series are generated by setting positive signs of  $q_i$   $i = 1, 2$ , whereas from panel (b), the negatively associated time series characteristics are produced by setting negative  $q_1$  and positive  $q_2$ . From panels (c) and (d), the cyclical fluctuations are confirmed when the parameter  $q_2$  has a negative sign.

Next, we investigated the CPACF of the MTD-AR(2) processes. Figure 2 shows the CPACF given by (18) for the same parameters used in Figure 1. Since the process is a second-order Markov, the CPACF with lags at greater than two vanish. The magnitude of the effect of the first two lag sequences is determined by the signs of the associated directions  $\mathbf{q}$  and mixing weight  $\mathbf{a}$ , and the concentration parameters in the binding density  $g$ .

The corresponding spectral density functions are plotted in Figure 3, where the parameters are the same as those used in the CACF plotted in Figure 1. The spectral densities plotted here have a mode at some frequencies, where these frequencies tell us the periodic patterns of time series fluctuations that are examined from the CACF plots in Figure 1.

The finite sample performance of the MLE is investigated using the same parameters used in the numerical examples. The true model was MTD-AR(2) with a wrapped Cauchy density function as its binding density. The parameter vector was chosen as  $\boldsymbol{\eta} = (a_1, \rho) = (0.3, 0.9)^T$ .

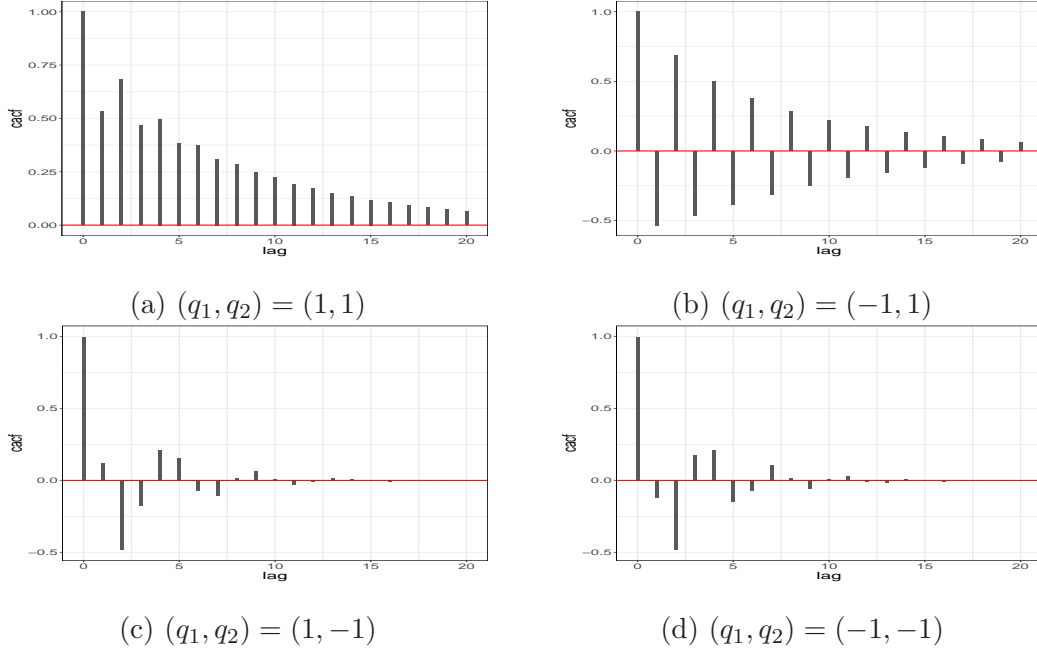


Figure 1: Plots of the CACF of the MTD-AR(2) processes with parameters  $a_1 = 0.3, a_2 = 0.7, \rho = 0.9$ , for panels (a)–(d), we set  $(q_1, q_2) = (1, 1), (q_1, q_2) = (-1, 1), (q_1, q_2) = (1, -1), (q_1, q_2) = (-1, -1)$ , respectively.

Recall that the mixing weight at lag 2 was  $a_2 = 1 - a_1 = 0.7$ . The direction of the dependency parameter vector  $q$  was set as  $(1, 1), (1, -1), (-1, 1)$ , and  $(-1, -1)$ . We drew a time series with length  $n \in \{250, 500, 1000\}$  from the MTD-AR(2) processes for the parameters given above.

First, we investigated the consistency and unbiased properties of the MLE for correctly specified cases, assuming that the autoregressive order of two with the true binding density  $g$  was known in advance. The simulations were conducted with 1000 repetitions, and we calculated the average and the root mean squared error (RMSE) of the estimates. Table 1 summarized the simulation results for the correctly specified case with known binding density  $g$  and autoregressive order  $p$ . From Table 1, as  $n$  increases, the RMSE decreases for all cases, which indicates the consistency results of the MLE. This was also confirmed that the bias of estimation decreases as  $n$  increases. The RMSEs for  $q = (1, 1)$  and  $(-1, 1)$  have larger values than those with  $q = (1, -1)$  and  $(-1, -1)$ . This is because the spectral density of the former case has higher peaks than that of the latter, as the larger area of the spectral density function yields larger variability in parameter estimation.

Second, we investigated a misspecified case so that the underlying binding density function was selected as a von Mises distribution while true binding density was wrapped Cauchy distribution whereas the autoregressive order is known in advance to be  $p = 2$ . In this setting,

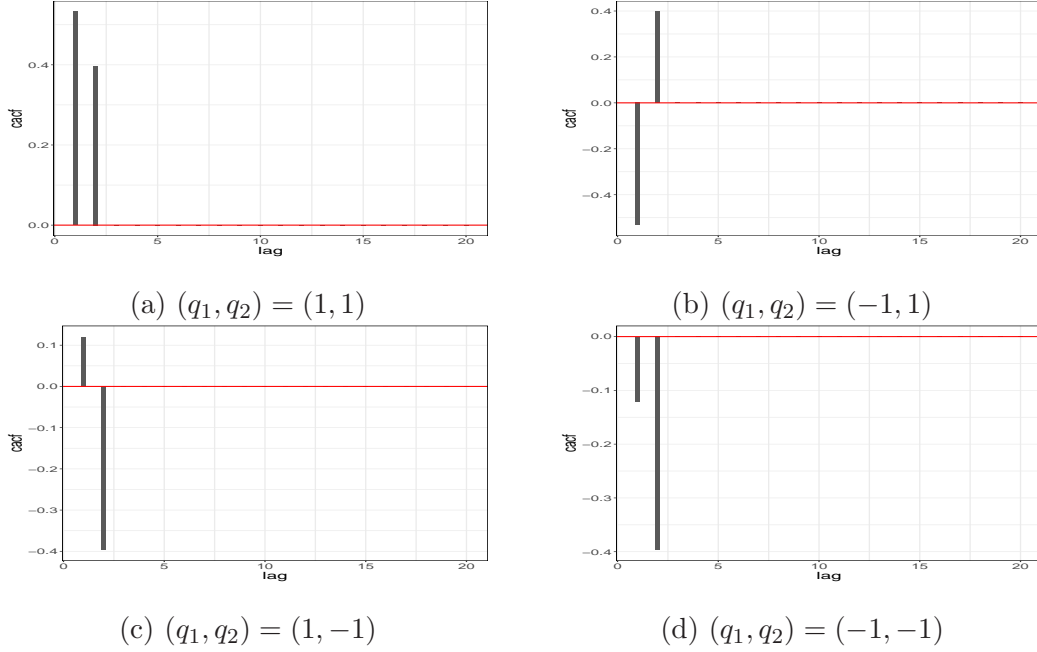


Figure 2: Plots of the CPACF of the MTD-AR(2) processes with parameters  $a_1 = 0.3, a_2 = 0.7, \rho = 0.9$ , for panels (a) to (d), we set  $(q_1, q_2) = (1, 1), (q_1, q_2) = (-1, 1), (q_1, q_2) = (1, -1), (q_1, q_2) = (-1, -1)$ , respectively.

the estimated concentration parameter  $\hat{\kappa}$  was transformed into the mean resultant length by  $\hat{\rho}_{VM} = I_1(\hat{\kappa})/I_0(\hat{\kappa})$ . Table 2 summarized the simulation results of the MLE when the true binding density  $g$  was wrapped Cauchy distribution while we applied von Mises distributions as the binding density in log-likelihood maximization. The parameter values were the same as those used in Table 1. According to Table 2, we can see that the RMSE has larger values compared with the values reported in Table 1, this was caused by the larger asymptotic variance of the misspecified model. Hence, we saw that the MLE for the misspecified case did not provide an efficient estimation for the model parameters, whereas this method can provide consistent estimates for the mixing weight parameters  $\hat{\mathbf{a}}$ .

Finally, we investigated the estimation results of the unknown autoregressive order. For this, we employ the Akaike information criterion (AIC) and Bayesian information criterion (BIC). Table 3 summarized the estimated autoregressive order  $p$  using AIC and BIC. The parameter values were chosen as the same parameters those used in Table 1. Since  $a_2 > a_1$ , no models were selected lags at 1 for all cases. We can observe that the BIC is the consistent estimator of  $\hat{p}$  as the ratio that the correct order model was selected increased as  $n$  increases, whereas the AIC worked worse than the BIC.

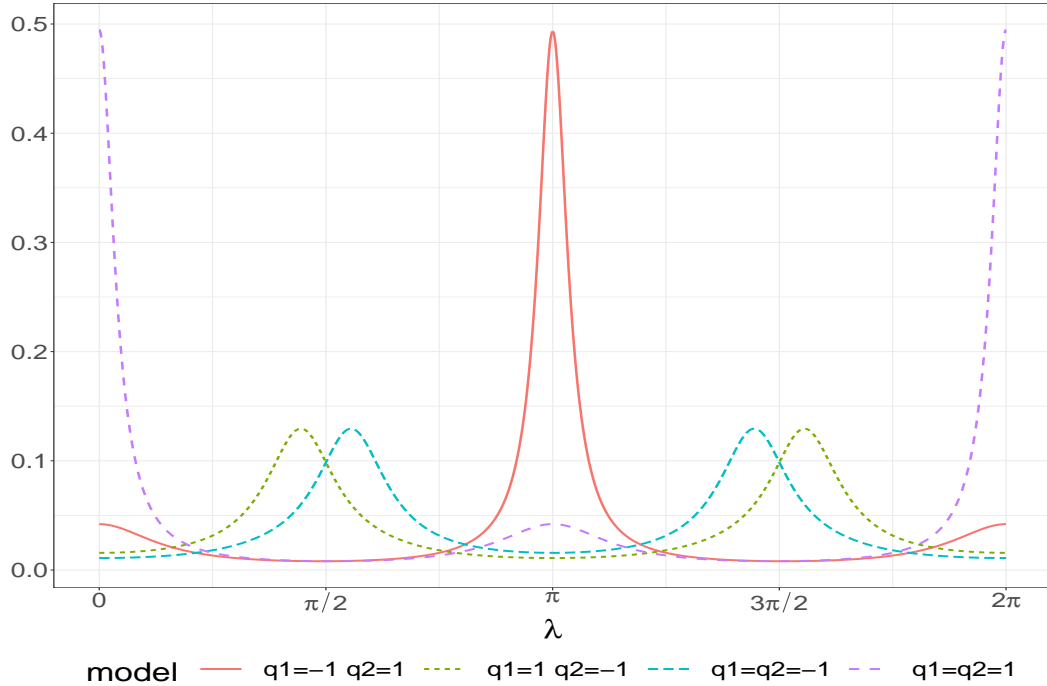


Figure 3: Plots of the spectral density function of MTD-AR(2) processes for  $(q_1, q_2) = (1, 1)$ ,  $(q_1, q_2) = (-1, 1)$ ,  $(q_1, q_2) = (1, -1)$ ,  $(q_1, q_2) = (-1, -1)$ . The parameters  $a_1, a_2$ , and  $\rho$  are the same as those used in Figure 1.

## 6 Data Analysis

We fitted MTD-AR( $p$ ) models for wind direction data which was investigated by [Agostinelli \(2007\)](#). The data consisted of 310 measurements of wind directions from January 29, 2001 to March 31, 2001, and the data were collected every 15 minutes from 3.00 am to 4.00 am. As can be confirmed from a time series plot shown in Figure 4, we saw that moderately positive autocorrelation existed and that was convinced from the sample CACF plotted in Figure 5. From Figure 5, we also observed that the negative circular autocorrelation existed at larger lags around 9 through 19. Figure 6 shows the sample CPACF of the observed time series. According to this figure, we can see a positive partial correlation at lag 1 and a weakly negative partial correlation at lag 4 exist, which makes the observed time series moderately periodic fluctuations.

Table 1: Simulation results for the maximum likelihood estimators.

| $q$        | $\hat{\alpha}_1$ |         |         |          | $\hat{\rho}$ |         |         |          |
|------------|------------------|---------|---------|----------|--------------|---------|---------|----------|
|            | (1, 1)           | (1, -1) | (-1, 1) | (-1, -1) | (1, 1)       | (1, -1) | (-1, 1) | (-1, -1) |
| $n = 250$  |                  |         |         |          |              |         |         |          |
| Mean       | 0.3031           | 0.3000  | 0.3050  | 0.3009   | 0.9001       | 0.8993  | 0.8998  | 0.9000   |
| RMSE       | 0.0470           | 0.0371  | 0.0509  | 0.0384   | 0.0089       | 0.0089  | 0.0092  | 0.0089   |
| $n = 500$  |                  |         |         |          |              |         |         |          |
| Mean       | 0.3014           | 0.3001  | 0.3001  | 0.2993   | 0.9001       | 0.8997  | 0.8993  | 0.9003   |
| RMSE       | 0.0337           | 0.0266  | 0.0329  | 0.0265   | 0.0065       | 0.0063  | 0.0065  | 0.0063   |
| $n = 1000$ |                  |         |         |          |              |         |         |          |
| Mean       | 0.3020           | 0.3007  | 0.3003  | 0.2991   | 0.9001       | 0.9001  | 0.9000  | 0.9000   |
| RMSE       | 0.0227           | 0.0191  | 0.0239  | 0.0183   | 0.0044       | 0.0044  | 0.0046  | 0.0045   |

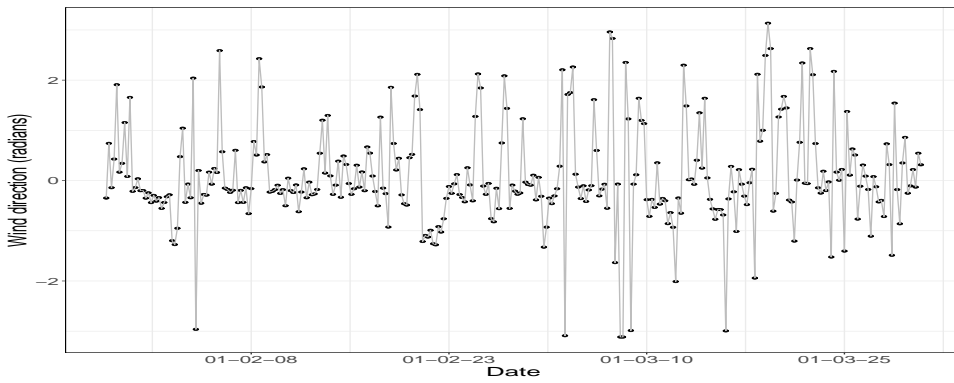


Figure 4: Time series plots for the wind direction at Col de la Roa in Italy.

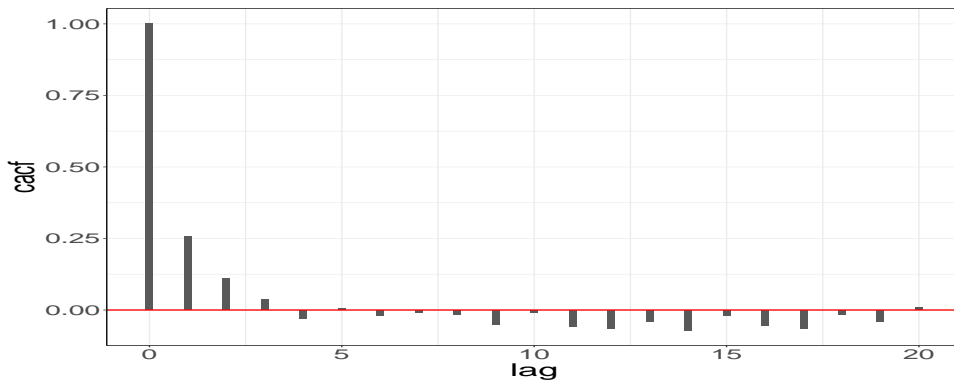


Figure 5: Sample CACF for the wind direction at Col de la Roa in Italy.

Table 2: Simulation results for the maximum likelihood estimates under the misspecified case.

| $q$        | $\hat{a}$ |         |         |          | $\hat{\rho}_{VM}$ |         |         |          |
|------------|-----------|---------|---------|----------|-------------------|---------|---------|----------|
|            | (1, 1)    | (1, -1) | (-1, 1) | (-1, -1) | (1, 1)            | (1, -1) | (-1, 1) | (-1, -1) |
| $n = 250$  |           |         |         |          |                   |         |         |          |
| Mean       | 0.2943    | 0.3009  | 0.2959  | 0.3020   | 0.9008            | 0.9107  | 0.9006  | 0.9119   |
| RMSE       | 0.0577    | 0.0379  | 0.0599  | 0.0400   | 0.0189            | 0.0218  | 0.0192  | 0.0219   |
| $n = 500$  |           |         |         |          |                   |         |         |          |
| Mean       | 0.2902    | 0.3009  | 0.2904  | 0.3030   | 0.8997            | 0.9118  | 0.8997  | 0.9125   |
| RMSE       | 0.0406    | 0.0279  | 0.0408  | 0.0275   | 0.0134            | 0.0183  | 0.0137  | 0.0179   |
| $n = 1000$ |           |         |         |          |                   |         |         |          |
| Mean       | 0.2875    | 0.3031  | 0.2883  | 0.3025   | 0.9002            | 0.9129  | 0.9004  | 0.9123   |
| RMSE       | 0.0301    | 0.0198  | 0.0317  | 0.0195   | 0.0094            | 0.0158  | 0.0096  | 0.0154   |

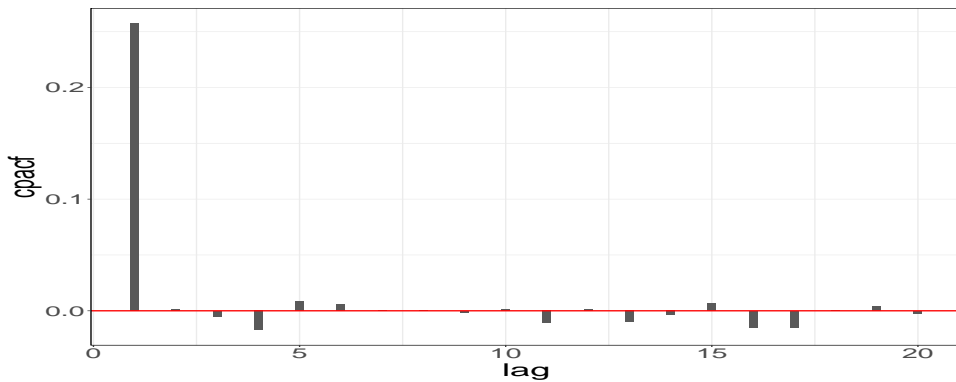


Figure 6: Sample CPACF for the wind direction at Col de la Roa in Italy.

The unknown autoregressive order  $p$  was determined by AIC and BIC, and we chose the wrapped Cauchy distribution as the binding density  $g$ . Figure 7 plots the values of AIC and BIC against maximum lags at seven. According to the figure, the lag order was selected at six from both AIC and BIC criteria.

Table 3: Selected AR orders by AIC and BIC.

|                         | $n = 250$ |     |     |     | $n = 500$ |     |     |     | $n = 1000$ |     |     |     |
|-------------------------|-----------|-----|-----|-----|-----------|-----|-----|-----|------------|-----|-----|-----|
| $p$                     | 1         | 2   | 3   | 4   | 1         | 2   | 3   | 4   | 1          | 2   | 3   | 4   |
| $\mathbf{q} = (1, 1)$   |           |     |     |     |           |     |     |     |            |     |     |     |
| AIC                     | 0         | 465 | 259 | 276 | 0         | 469 | 249 | 282 | 0          | 481 | 284 | 235 |
| BIC                     | 0         | 775 | 162 | 63  | 0         | 818 | 142 | 40  | 0          | 850 | 124 | 26  |
| $\mathbf{q} = (1, -1)$  |           |     |     |     |           |     |     |     |            |     |     |     |
| AIC                     | 0         | 456 | 262 | 282 | 0         | 478 | 268 | 254 | 0          | 483 | 259 | 258 |
| BIC                     | 0         | 762 | 155 | 83  | 0         | 805 | 146 | 49  | 0          | 869 | 100 | 31  |
| $\mathbf{q} = (-1, 1)$  |           |     |     |     |           |     |     |     |            |     |     |     |
| AIC                     | 0         | 415 | 275 | 310 | 0         | 463 | 240 | 297 | 0          | 467 | 270 | 263 |
| BIC                     | 0         | 742 | 159 | 99  | 0         | 806 | 129 | 65  | 0          | 845 | 112 | 43  |
| $\mathbf{q} = (-1, -1)$ |           |     |     |     |           |     |     |     |            |     |     |     |
| AIC                     | 0         | 464 | 231 | 305 | 0         | 442 | 261 | 297 | 0          | 467 | 287 | 246 |
| BIC                     | 0         | 775 | 142 | 83  | 0         | 806 | 130 | 64  | 0          | 860 | 104 | 36  |

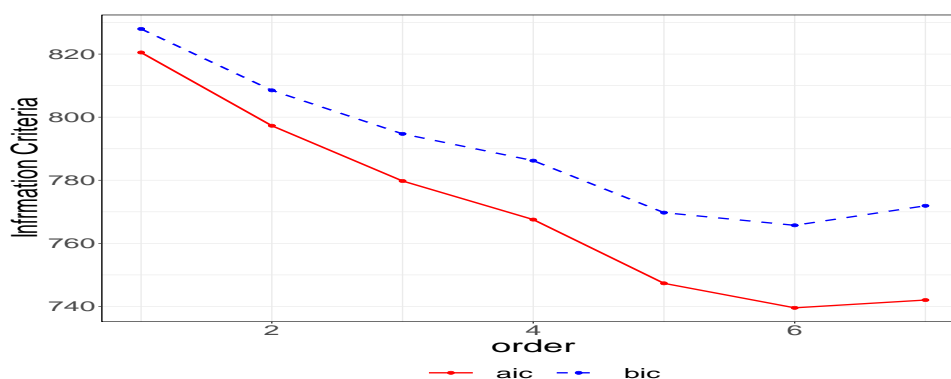


Figure 7: Plots of the AIC and BIC for fitted MTD-AR( $p$ ) models with  $p = 1, \dots, 7$ .

Table 4 summarized the estimated parameters with mixture weights, the concentration of the binding density  $g$ , and the signs of the directions of the dependency at lags from 1 through 7. The estimated  $\hat{q}_i$ s were denoted with signs in the parenthesis, where (+) and (-) indicate  $\hat{q}_i = +1$  and  $\hat{q}_i = -1$ , respectively. Recall that the MTD-AR( $p$ ) models with lag order  $p = 6$  were selected as the best model among lags from 1 to 7.

The log periodogram for the circular time series together with its smoothed estimates

Table 4: Estimated mixture weights together with the directions of the dependency at lags from 1 through 7.

| $p$ | $\hat{a}_1$ | $\hat{a}_2$ | $\hat{a}_3$ | $\hat{a}_4$ | $\hat{a}_5$ | $\hat{a}_6$ | $\hat{a}_7$ | $\hat{\rho}$ |
|-----|-------------|-------------|-------------|-------------|-------------|-------------|-------------|--------------|
| 1   | 1.000       |             |             |             |             |             |             | 0.642        |
| 2   | (+)0.744    | (+)0.256    |             |             |             |             |             | 0.689        |
| 3   | (+)0.654    | (+)0.186    | (-)0.160    |             |             |             |             | 0.721        |
| 4   | (+)0.599    | (+)0.118    | (+)0.119    | (+)0.164    |             |             |             | 0.736        |
| 5   | (+)0.545    | (+)0.092    | (+)0.087    | (-)0.085    | (+)0.191    |             |             | 0.760        |
| 6   | (+)0.514    | (+)0.086    | (+)0.072    | (-)0.085    | (+)0.160    | (+)0.083    |             | 0.755        |
| 7   | (+)0.508    | (+)0.082    | (+)0.069    | (+)0.086    | (+)0.153    | (+)0.069    | (+)0.032    | 0.773        |

and log spectral density function for the fitted MTD-AR(6) are illustrated in Figure 8. The fitted MTD-AR(6) spectral density function performs well in capturing observed spectra, which can be confirmed by comparing log-smoothed periodogram.

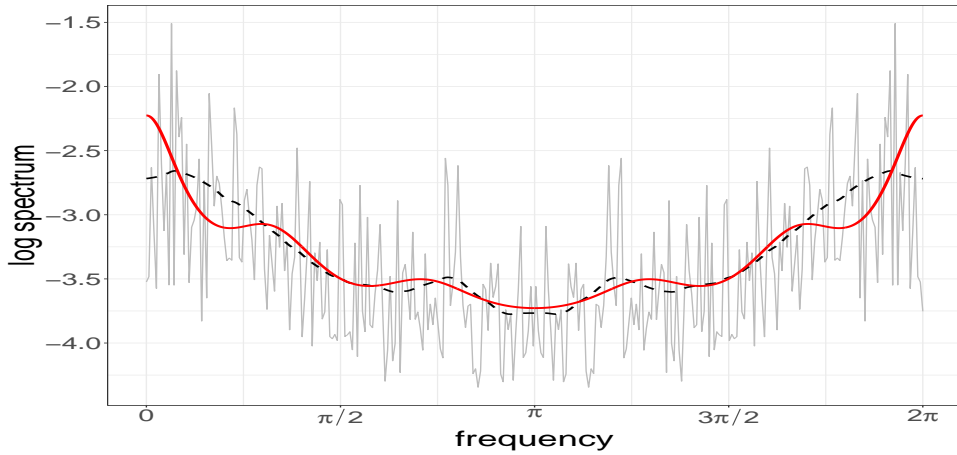


Figure 8: Plots of the circular periodogram, its smoothed estimates (dashed line) and the spectral density function of the fitted MTD-AR(6) model (solid line).

## 7 Conclusion

This study proposed a higher-order Markov model on the circle by incorporating a mixture of transition density modeling approach. Statistical properties including first- and second-order stationarity together with CACF and CPACF are derived. In addition, the spectral density function of the circular time series processes is obtained by assuming the location parameter of the binding density is fixed at  $\mu = 0$ . For the parameter estimation, the MLE is introduced

and its asymptotic properties are provided. These theoretical results are investigated by a numerical illustration using the MTD-AR(2) process and some Monte Carlo simulations are conducted to verify the finite sample performance of the MLEs. The limitation of the proposed models includes that the explicit expressions for the spectral density function are for the case with  $\mu = 0$ , while for the general case with  $\mu \neq 0$ , the CACF together with the spectral density function have complicated forms. These problems remain as future work. In addition, non-parametric spectral density function estimators are worth investigating.

## Acknowledgments

Hiroaki Ogata was supported in part by JSPS KAKENHI Grant Number 18K11193. Takayuki Shiohama was supported in part by JSPS KAKENHI Grant Number 22K11944, and Nanzan University Pache Research I-A-2 for the 2023 academic year.

## References

- Abe, T., H. Ogata, T. Shiohama, and H. Taniyai (2017). Circular autocorrelation of stationary circular Markov processes. *Statistical Inference for Stochastic Processes* 20(3), 275–290.
- Agostinelli, C. (2007). Robust estimation for circular data. *Computational Statistics & Data Analysis* 51(12), 5867–5875.
- Berchtold, A. and A. E. Raftery (2002). The mixture transition distribution model for high-order Markov chains and non-gaussian time series. *Statistical Science* 17(3), 328–356.
- Breckling, J. (1989). *The analysis of directional time series: applications to wind speed and direction*, Volume 61 of *Lecture Notes in Statistics*. Springer Science & Business Media.
- Degerine, S. (1990). Canonical partial autocorrelation function of a multivariate time series. *The Annals of Statistics*, 961–971.
- Douc, R., E. Moulines, and D. Stoffer (2014). *Nonlinear Time Series: Theory, Methods and Applications with R Examples*. CRC Press.
- Fisher, N. I. and A. J. Lee (1983). A correlation coefficient for circular data. *Biometrika* 70(2), 327–332.
- Fisher, N. I. and A. J. Lee (1994). Time series analysis of circular data. *Journal of the Royal Statistical Society: Series B (Methodological)* 56(2), 327–339.

- Holzmann, H., A. Munk, M. Suster, and W. Zucchini (2006). Hidden Markov models for circular and linear-circular time series. *Environmental and Ecological Statistics* 13(3), 325–347.
- Jammalamadaka, S. R. and A. SenGupta (2001). *Topics in Circular Statistics*. World Scientific.
- Jones, M., A. Pewsey, and S. Kato (2015). On a class of circular copulas for circular distributions. *Annals of the Institute of Statistical Mathematics* 67(5), 843–862.
- Kato, S. (2010). A Markov process for circular data. *Journal of the Royal Statistical Society: Series B (Statistical Methodology)* 72(5), 655–672.
- Le, N. D., R. D. Martin, and A. E. Raftery (1996). Modeling flat stretches, bursts outliers in time series using mixture transition distribution models. *Journal of the American Statistical Association* 91(436), 1504–1515.
- Mardia, K. V. and P. E. Jupp (2009). *Directional Statistics*. Chichester: John Wiley & Sons.
- Morf, M., A. Vieira, and T. Kailath (1978). Covariance characterization by partial autocorrelation matrices. *The Annals of Statistics*, 643–648.
- Pewsey, A. and E. García-Portugués (2021). Recent advances in directional statistics. *Test* 30(1), 1–58.
- Pewsey, A., M. Neuhäuser, and G. D. Ruxton (2013). *Circular Statistics in R*. Oxford University Press.
- Raftery, A. E. (1985). A model for high-order Markov chains. *Journal of the Royal Statistical Society: Series B (Methodological)* 47(3), 528–539.
- Raftery, A. E. and S. Tavaré (1994). Estimation and modelling repeated patterns in high order Markov chains with the mixture transition distribution model. *Journal of the Royal Statistical Society: Series C (Applied Statistics)* 43(1), 179–199.
- Wehrly, T. E. and R. A. Johnson (1980). Bivariate models for dependence of angular observations and a related Markov process. *Biometrika* 67(1), 255–256.
- Wei, W. W. (1990). *Time Series Analysis: Univariate and Multivariate Methods*. Wiley.

## A Appendix

In this appendix, we will provide all proofs of the theorems and lemmas stated in Sections 3 and 4. Now, we give the following lemmas.

**Lemma 1.** *Let  $g$  be an arbitrary circular density satisfying Assumption 1. Then*

$$\int_{\Pi} \begin{pmatrix} \cos m\theta_j \\ \sin m\theta_j \end{pmatrix} g(\theta_j - q_i\theta_{j-i}) d\theta_j = D_m Q_i \begin{pmatrix} \cos m\theta_{j-i} \\ \sin m\theta_{j-i} \end{pmatrix},$$

where  $\Pi = (-\pi, \pi]$ ,

$$D_m = \rho_m \begin{pmatrix} \cos \mu_m & -\sin \mu_m \\ \sin \mu_m & \cos \mu_m \end{pmatrix}, \quad Q_i = \begin{pmatrix} 1 & 0 \\ 0 & q_i \end{pmatrix},$$

and  $q_i \in \{-1, 1\}$  is a constant,  $\rho_m$  and  $\mu_m$  are the resultant length and direction of  $m$ th order trigonometric moment of the circular density function  $g$ .

**Proof** Direct calculation yields the following result.

$$\begin{aligned} & \int_{\Pi} \begin{pmatrix} \cos m\theta_j \\ \sin m\theta_j \end{pmatrix} g(\theta_j - q_i\theta_{j-i}) d\theta_j \\ &= \int_{\Pi} \begin{pmatrix} \cos m(s + q_i\theta_{j-i}) \\ \sin m(s + q_i\theta_{j-i}) \end{pmatrix} g(s) ds \\ &= \int_{\Pi} \begin{pmatrix} \cos ms \cos(q_i m\theta_{j-i}) - \sin ms \sin(q_i m\theta_{j-i}) \\ \sin ms \cos(q_i m\theta_{j-i}) + \cos ms \sin(q_i m\theta_{j-i}) \end{pmatrix} g(s) ds \\ &= \int_{\Pi} \begin{pmatrix} \cos ms & -\sin ms \\ \sin ms & \cos ms \end{pmatrix} g(s) ds \begin{pmatrix} \cos q_i m\theta_{j-i} \\ \sin q_i m\theta_{j-i} \end{pmatrix} \\ &= D_m Q_i \begin{pmatrix} \cos m\theta_{j-i} \\ \sin m\theta_{j-i} \end{pmatrix}, \end{aligned}$$

where we use a transformation of variable in the second equation with  $s = \theta_j - q_i\theta_{j-i}$  and  $ds = d\theta_j$ . □

**Lemma 2.** *Let  $g$  be an arbitrary circular density. Then*

$$\int_{\Pi} \begin{pmatrix} \cos m\theta_j & \sin m\theta_j \\ \sin m\theta_j & -\cos m\theta_j \end{pmatrix} g(\theta_j - q_i\theta_{j-i}) d\theta_j = D_m Q_i \begin{pmatrix} \cos m\theta_{j-i} & \sin m\theta_{j-i} \\ \sin m\theta_{j-i} & -\cos m\theta_{j-i} \end{pmatrix} Q_i,$$

where  $D_m$  and  $Q_i$  are the same matrices defined in Lemma 1.

**Proof** Similar to the proof of Lemma 1, we have

$$\begin{aligned}
& \int_{\Pi} \begin{pmatrix} \cos m\theta_j & \sin m\theta_j \\ \sin m\theta_j & -\cos m\theta_j \end{pmatrix} g(\theta_j - q_i\theta_{j-i}) d\theta_j \\
&= \int_{\Pi} \begin{pmatrix} \cos m(s + q_i\theta_{j-i}) & \sin m(s + q_i\theta_{j-i}) \\ \sin m(s + q_i\theta_{j-i}) & -\cos m(s + q_i\theta_{j-i}) \end{pmatrix} g(s) ds \\
&= \int_{\Pi} \begin{pmatrix} \cos ms & -\sin ms \\ \sin ms & \cos ms \end{pmatrix} g(s) ds \begin{pmatrix} \cos q_i m\theta_{j-i} & \sin q_i m\theta_{j-i} \\ \sin q_i m\theta_{j-i} & -\cos q_i m\theta_{j-i} \end{pmatrix} \\
&= D_m Q_i \begin{pmatrix} \cos m\theta_{j-i} & \sin m\theta_{j-i} \\ \sin m\theta_{j-i} & -\cos m\theta_{j-i} \end{pmatrix} Q_i.
\end{aligned}$$

□

**Proof of Theorem 2** See, for example, (Wei, 1990, Theorem 2.7.1) for the results of difference equations. □

**Proof of Theorem 3** Recall Assumption 2 ensures the diagonal covariance matrices  $\Gamma_j = \Gamma_{-j} = \text{diag}(\gamma_{j,11}, \gamma_{j,22})$ . Then, the linear systems (15) and (16) become identical:

$$\begin{bmatrix} \Gamma_0 & \Gamma_1 & \cdots & \Gamma_{s-1} \\ \Gamma_1 & \Gamma_0 & \cdots & \Gamma_{s-2} \\ \vdots & \vdots & \ddots & \vdots \\ \Gamma_{s-1} & \Gamma_{s-2} & \cdots & \Gamma_0 \end{bmatrix} \begin{bmatrix} \Xi_1 \\ \Xi_2 \\ \vdots \\ \Xi_s \end{bmatrix} = \begin{bmatrix} \Gamma_1 \\ \Gamma_2 \\ \vdots \\ \Gamma_s \end{bmatrix}. \quad (24)$$

Note that the all roots of (24) are also diagonal matrices, which can be written as  $\Xi_j = \text{diag}(\xi_{j,11}, \xi_{j,22})$ . Then, the linear system (24) decomposes into two systems

$$\begin{bmatrix} \gamma_{0,11} & \gamma_{1,11} & \cdots & \gamma_{s-1,11} \\ \gamma_{1,11} & \gamma_{0,11} & \cdots & \gamma_{s-2,11} \\ \vdots & \vdots & \ddots & \vdots \\ \gamma_{s-1,11} & \gamma_{s-2,11} & \cdots & \gamma_{0,11} \end{bmatrix} \begin{bmatrix} \xi_{1,11} \\ \xi_{2,11} \\ \vdots \\ \xi_{s,11} \end{bmatrix} = \begin{bmatrix} \gamma_{1,11} \\ \gamma_{2,11} \\ \vdots \\ \gamma_{s,11} \end{bmatrix}$$

and

$$\begin{bmatrix} \gamma_{0,22} & \gamma_{1,22} & \cdots & \gamma_{s-1,22} \\ \gamma_{1,22} & \gamma_{0,22} & \cdots & \gamma_{s-2,22} \\ \vdots & \vdots & \ddots & \vdots \\ \gamma_{s-1,22} & \gamma_{s-2,22} & \cdots & \gamma_{0,22} \end{bmatrix} \begin{bmatrix} \xi_{1,22} \\ \xi_{2,22} \\ \vdots \\ \xi_{s,22} \end{bmatrix} = \begin{bmatrix} \gamma_{1,22} \\ \gamma_{2,22} \\ \vdots \\ \gamma_{s,22} \end{bmatrix}.$$

Now, under Assumption 2, (17) becomes

$$\psi_s^{(C)} = \frac{(\gamma_{s,11} - \xi_{1,11}\gamma_{s-1,11} - \cdots - \xi_{s-1,11}\gamma_{1,11})}{(\gamma_{0,11} - \xi_{1,11}\gamma_{1,11} - \cdots - \xi_{s-1,11}\gamma_{s-1,11})} \times \frac{(\gamma_{s,22} - \xi_{1,22}\gamma_{s-1,22} - \cdots - \xi_{s-1,22}\gamma_{1,22})}{(\gamma_{0,22} - \xi_{1,22}\gamma_{1,22} - \cdots - \xi_{s-1,22}\gamma_{s-1,22})}.$$

Similar to the result of (Wei, 1990, Section 2.3), it reduces to

$$\psi_s^{(C)} = \frac{\begin{vmatrix} \gamma_{0,11} & \gamma_{1,11} & \cdots & \gamma_{s-2,11} & \gamma_{1,11} \\ \gamma_{1,11} & \gamma_{0,11} & \cdots & \gamma_{s-3,11} & \gamma_{2,11} \\ \vdots & \vdots & & \vdots & \vdots \\ \gamma_{s-1,11} & \gamma_{s-2,11} & \cdots & \gamma_{1,11} & \gamma_{s,11} \end{vmatrix} \begin{vmatrix} \gamma_{0,22} & \gamma_{1,22} & \cdots & \gamma_{s-2,22} & \gamma_{1,22} \\ \gamma_{1,22} & \gamma_{0,22} & \cdots & \gamma_{s-3,22} & \gamma_{2,22} \\ \vdots & \vdots & & \vdots & \vdots \\ \gamma_{s-1,22} & \gamma_{s-2,22} & \cdots & \gamma_{1,22} & \gamma_{s,22} \end{vmatrix}}{\begin{vmatrix} \gamma_{0,11} & \gamma_{1,11} & \cdots & \gamma_{s-2,11} & \gamma_{s-1,11} \\ \gamma_{1,11} & \gamma_{0,11} & \cdots & \gamma_{s-3,11} & \gamma_{s-2,11} \\ \vdots & \vdots & & \vdots & \vdots \\ \gamma_{s-1,11} & \gamma_{s-2,11} & \cdots & \gamma_{1,11} & \gamma_{0,11} \end{vmatrix} \begin{vmatrix} \gamma_{0,22} & \gamma_{1,22} & \cdots & \gamma_{s-2,22} & \gamma_{s-1,22} \\ \gamma_{1,22} & \gamma_{0,22} & \cdots & \gamma_{s-3,22} & \gamma_{s-2,22} \\ \vdots & \vdots & & \vdots & \vdots \\ \gamma_{s-1,22} & \gamma_{s-2,22} & \cdots & \gamma_{1,22} & \gamma_{0,22} \end{vmatrix}},$$

which is identical to (18).  $\square$

**Proof of Theorem 4** Let  $X_{1,t}$  and  $X_{2,t}$  be two stationary AR( $p$ ) processes, defined as

$$\phi_1(B)X_{1,t} = \tilde{u}_{1,t} \quad \text{and} \quad \phi_2(B)X_{2,t} = \tilde{u}_{2,t},$$

where  $\tilde{u}_{1,t}$  and  $\tilde{u}_{2,t}$  are uncorrelated processes with zero means, and some constant variances  $\sigma_{\tilde{u}_1}^2$  and  $\sigma_{\tilde{u}_2}^2$ , respectively. Then, the autocovariances of  $X_{1,t}$  and  $X_{2,t}$  also satisfies (14), which is representing the autocovariance relationships of  $\cos \Theta_t$  and  $\sin \Theta_t$ . From the second-order stationarity of the processes  $X_{1,t}$  and  $X_{2,t}$ , we have

$$\text{var}(X_{1,t}) = \frac{\sigma_{\tilde{u}_1}^2}{1 - 2\rho_1 \sum_{i=1}^p a_i \gamma_{i,11}}$$

and

$$\text{var}(X_{2,t}) = \frac{\sigma_{\tilde{u}_2}^2}{1 - 2\rho_1 \sum_{i=1}^p q_i a_i \gamma_{i,22}}.$$

Since the circular uniform marginal assumption of  $f$ , we have  $\text{var}(\cos \Theta_t) = \text{var}(\sin \Theta_t) = 1/2$ . Therefore, if we set  $\text{var}(X_{1,t}) = \text{var}(X_{2,t}) = 1/2$ , that is, if we set

$$\sigma_{\tilde{u}_1}^2 = \frac{1 - 2\rho_1 \sum_{i=1}^p a_i \gamma_{i,11}}{2} \quad \text{and} \quad \sigma_{\tilde{u}_2}^2 = \frac{1 - 2\rho_1 \sum_{i=1}^p q_i a_i \gamma_{i,22}}{2},$$

the processes  $X_{1,t}$  and  $X_{2,t}$  have the completely same autocovariance structures as those of the processes  $\cos \Theta_t$  and  $\sin \Theta_t$ , respectively. Then the spectral densities for the process  $\cos \Theta_t$  and  $\sin \Theta_t$  are the same as those of the processes  $X_{1,t}$  and  $X_{2,t}$ , which are

$$f_{X_1}(\omega) = \frac{1 - 2\rho_1 \sum_{i=1}^p a_i \gamma_{i,11}}{4\pi |\phi_1(e^{-i\omega})|^2}$$

and

$$f_{X_2}(\omega) = \frac{1 - 2\rho_1 \sum_{i=1}^p q_i a_i \gamma_{i,22}}{4\pi |\phi_2(e^{-i\omega})|^2}.$$

Using the convolution theorem of Fourier transforms, the  $k$ -th circular autocovariance function becomes

$$\begin{aligned}\gamma_{k,11}\gamma_{k,22} &= \left( \int_{-\pi}^{\pi} e^{ik\omega_1} f_{X_1}(\omega_1) d\omega_1 \right) \left( \int_{-\pi}^{\pi} e^{ik\omega_2} f_{X_2}(\omega_2) d\omega_2 \right) \\ &= \int_{-\pi}^{\pi} \left( \int_{-\pi}^{\pi} f_{X_1}(\omega_1) f_{X_2}(\omega_2 - \omega_1) d\omega_1 \right) e^{ik\omega_2} d\omega_2.\end{aligned}$$

This implies the spectral density of  $\Theta_t$  is expressed as that in the theorem.  $\square$

**Proof of Theorem 5** Since the first- and second-order stationarity results stated by Theorems 1 and 2 together with the definition of the Markov kernel density (3) and its autocovariance function is absolutely summable such that  $\sum_{k=-\infty}^{\infty} |\det \Gamma_k| < \infty$ , the process (3) is strictly stationary and ergodic. The strongly consistent result follows from (Douc et al., 2014, Theorem 8.7), since Assumption 2(b) and (c) imply that the Markov kernel density defined by (3) is continuous and its logarithm is bounded above by  $\sup_{\eta \in \mathcal{H}} E_{\eta_0} \{ \ln(\sum_{i=1}^p a_i g(\Theta_t - q_{i0} \Theta_{t-i}; \rho)) \} < \infty$ .  $\square$

**Proof of Theorem 6** From Assumption 3(b), the continuity of  $g(\cdot)$  implies  $\sum_{i=1}^p a_i g(\theta_t - q_{i0} \theta_{t-i}; \rho)$  is continuous which yields following

$$\left. \frac{\partial}{\partial \boldsymbol{\eta}} \ell_n(\boldsymbol{\eta}, \mathbf{q}_0) \right|_{\hat{\boldsymbol{\eta}}_n} = \mathbf{0}.$$

In addition, we observe the following expansion as

$$\left. \frac{\partial}{\partial \boldsymbol{\eta}} \ell_n(\boldsymbol{\eta}, \mathbf{q}_0) \right|_{\boldsymbol{\eta}_0} + \left. \frac{\partial^2}{\partial \boldsymbol{\eta} \partial \boldsymbol{\eta}^T} \ell_n(\boldsymbol{\eta}, \mathbf{q}_0) \right|_{\boldsymbol{\eta}_*} (\hat{\boldsymbol{\eta}}_n - \boldsymbol{\eta}_0) = \mathbf{0},$$

where  $\boldsymbol{\eta}_*$  satisfies  $\|\boldsymbol{\eta}_* - \boldsymbol{\eta}_0\| \leq \|\hat{\boldsymbol{\eta}}_n - \boldsymbol{\eta}_0\|$ . Then we observe

$$\sqrt{n}(\hat{\boldsymbol{\eta}}_n - \boldsymbol{\eta}_0) = \left[ -\frac{1}{n} \left. \frac{\partial^2}{\partial \boldsymbol{\eta} \partial \boldsymbol{\eta}^T} \ell_n(\boldsymbol{\eta}, \mathbf{q}_0) \right|_{\boldsymbol{\eta}_*} \right]^{-1} \left. \frac{1}{\sqrt{n}} \frac{\partial}{\partial \boldsymbol{\eta}} \ell_n(\boldsymbol{\eta}, \mathbf{q}_0) \right|_{\boldsymbol{\eta}_0}.$$

Using a law of large numbers, we have

$$-\frac{1}{n} \left. \frac{\partial^2}{\partial \boldsymbol{\eta} \partial \boldsymbol{\eta}^T} \ell_n(\boldsymbol{\eta}, \mathbf{q}_0) \right|_{\boldsymbol{\eta}_*} \rightarrow_p I(\boldsymbol{\eta}_0)$$

where  $I(\boldsymbol{\eta}_0)$  is defined by Assumption 3(d). A central limit theorem implies

$$\frac{1}{\sqrt{n}} \left. \frac{\partial}{\partial \boldsymbol{\eta}} \ell_n(\boldsymbol{\eta}, \mathbf{q}_0) \right|_{\boldsymbol{\eta}_0} \xrightarrow{d} N(\mathbf{0}, \mathbf{J}(\boldsymbol{\eta}_0)),$$

see, for details, (Douc et al., 2014, Theorem 8.13). This together with Slutsky's lemma completes the proof of the theorem.  $\square$